

Contents lists available at ScienceDirect

# **Marine Structures**

journal homepage: www.elsevier.com/locate/marstruc



# CFD and experimental assessment of green water events on an FPSO hull section in beam waves



Guilherme F. Rosetti<sup>a,\*</sup>, Mariana L. Pinto<sup>a,b</sup>, Pedro C. de Mello<sup>a,b</sup>, Claudio M.P. Sampaio<sup>a,b</sup>, Alexandre N. Simos<sup>b</sup>, Daniel F.C. Silva<sup>c</sup>

#### ARTICLE INFO

# Keywords: CFD analysis FPSO Green water prediction Beam waves Deck impact loads

#### ABSTRACT

CFD prediction of water on deck and impact on a deck structure is investigated and results confronted to those obtained in a wave flume. A simplified set-up is employed, consisting of a model of an FPSO section fixed in the flume, emulating its interaction with regular beam waves. The influence of a riser balcony is also considered. The aim is to focus the investigation on the ability to reproduce the dynamics of the water shipping on FPSOs. In addition, the tests in regular waves allowed an evaluation of variations from cycle to cycle, making the apparent randomness of the maximum impact loads more evident. An analysis is made on the main factors that control these variations and how they are affected by changes in the wave parameters. Apart from the variability, results show that the CFD simulations were generally able to predict the statistical maxima with sufficient accuracy, even for situations with large volumes of water on deck. Even though the discrepancies on the force maxima rise for the steepest waves, results attest that the force impulses remain accurate.

# 1. Introduction

Green water events represent an important risk for the operations of moored FPSOs, which means that the vessel is not able to weathervane. The water columns rising over the freeboard may reach several meters and resulting impacts can be quite severe from the side. Although with low probability of occurrence, these events may impose serious damage to deck structures.

An extensive range of works is available on the subject and Silva [1–3] has carried out a survey of publications based on experimental, analytical and numerical results, providing a good overview of the recent literature in this field. Within the publications dealing with FPSOs, most is concerned with water elevations in head and oblique waves and a rather smaller number of works addresses the problem in beam waves. In the Brazilian context, for instance, most of the new FPSOs rely on spread-mooring systems (SMS) for station keeping. Contrary to those based on turrets, the ability these vessels have to weathervane is quite restricted, and green water events in beam sea (or nearly beam sea) scenarios become possible. In early publications [4–6], it was common to find model tests with FPSOs that included models of the real mooring and risers systems subjected to irregular waves (and sometimes also current and wind [5]), which is an overly complex situation to develop a fundamental understanding on how to determine: i) the water elevations and water shipping pattern for each wave condition; ii) the impact forces in each event; iii) post-impact behavior. Perhaps for that reason, a growing number of publications using CFD and regular waves is observed in more recent years [6–8] which

E-mail address: gfeitosarosetti@usp.br (G.F. Rosetti).

<sup>&</sup>lt;sup>a</sup> Numerical Offshore Tank - University of São Paulo, Brazil

<sup>&</sup>lt;sup>b</sup> Dept. of Naval Architecture and Ocean Engineering - University of São Paulo, Brazil

c CENPES/Petrobras, Brazil

<sup>\*</sup> Corresponding author.

G.F. Rosetti et al. Marine Structures 65 (2019) 154-180

reflects the need of deeper fundamental knowledge regarding this phenomenon. Among the different aspects concerning green water events, efforts are directed to a better understanding of the following issues: the conditions under which water exceeds the freeboard, as well as how the flow behaves after these events both in fixed and moving structures; water propagation on deck; water impact on deck structures; mitigation measures; statistical approaches to predict critical events, among others.

A fundamental study combining experimental, numerical and analytical approaches was presented in Ref. [9]. The floater shape and bow curvature have been varied to investigate their effects on the green water patterns. Beam waves green water events are also preliminarily studied. Empirical and numerical approaches are used to estimate and correlate the water elevations, propagation on deck and impacts on deck structures. A large number of model tests are used to calibrate the predictions. Different qualitative behaviors of water embarkment are identified; the most frequent ones can be associated to the well-known dam-break and plunging + dam-break types of events, and less frequently more intense events that resemble the so-called hammer-fist events [10] are also observed.

In search of deeper phenomenological knowledge, Greco [10] numerically investigated a number of parameters influencing green water in two-dimensional studies: the main ship dimensions, freeboard values, hull shape, presence of bulb, wave parameters and influence of body motions. Freeboard height, wave steepness and relative motions of the structure are identified as major contributors to green-water loading.

An important experimental benchmark to numerical and empirical studies was provided in Ref. [8], in which the bow of a captive FPSO was exposed to regular waves. The water impacts forces on deck structures and water elevations were presented. Conversely, the water elevation on an FPSO in head, beam and oblique seas were studied and the results were compared to different probability distributions in Ref. [4]. Similarly, in search of statistical representation to wave elevations, the works in Refs. [6,11] investigated different probability density distributions.

In most studies, hull appendices have not been considered in the model tests and calculations. However, in Ref. [9] the impact forces are studied for a number of hulls and different breakwaters, concluding that the loading is strongly dependent upon shape and position of the breakwater. Ref. [12] presents a study in which V-shaped breakwaters show adequate behavior in preventing impact with other deck structures. In Ref. [13], a parametric study is carried out with a vane-type protection concluding that impact attenuation may range from 30% to 70% depending on its geometry. Finally, in Ref. [14] a deflector is fitted on top of the side of a gravity-based structure and it indeed tends to deflect the jet away from the deck. This is a relevant observation because a similar geometric structure, namely the rise balcony, is investigated herein.

CFD has been applied to study different aspects of the green water phenomenon. One may refer, for example, to Refs. [3,7,11,3,15], among others. The RANS + VOF approach has performed properly to study this problem, despite its strong nonlinearity and complexity. Nonetheless, consideration of all the aspects, such as the simulation of random waves and moving bodies is still restricted by the practical limits of this powerful tool. The comparison of CFD and model tests results for a better understanding of the phenomenon in a simplified set-up is the main motivation for the current work.

The main objective of this paper is to study the water shipping and impacts events in beam waves in detail (elevations, impact forces, force impulse, velocity above the deck and flow patterns). With this purpose, regular waves of different heights and steepnesses are driven in a flume over a two-dimensional fixed model representing the cross section of an FPSO. There is also an interest in investigating whether the presence of a riser balcony (see an illustration of a riser balcony in an FPSO in Fig. 1) would influence the water shipping and impact on deck structures. Therefore, models with and without a thin plate representing this particular riser balcony are considered.

Experiments and CFD calculations were combined in the present work for consistency checks and for obtaining information about the phenomena at play. Experiments were carried out in a wave flume, considering a scale factor of 1:180. Regular waves were tested with wave steepness of 4%, 6% and 8%, wave heights varying from 17 mm to 117 mm (3.06m and 21.09m in prototype scale) and periods from 0.52s to 0.97s (7s and 13s in prototype scale). In all tests, the freeboard was set to 31 mm (5.58m in prototype scale), therefore some of the tests presented wave amplitudes much larger than the freeboard. Evidently, these cases do not necessarily



Fig. 1. Picture of the Petrobras P66 FPSO showing the riser balcony [16].



Fig. 2. Wave generation (a) and absorption (b) systems.

correspond to real expected conditions, but they are explored in order to investigate the water shipping events of highly nonlinear waves and the ability of the CFD model for capturing these events correctly.

Sections 2 and 3 respectively present the experimental and numerical set-ups adopted for this study. Next, Sec. 4 brings the comparison of the results obtained from model tests and CFD calculations, followed by a more detailed analysis of selected cases in Sec. 5. Finally, Sec. 6 draws the main conclusions obtained in this work.

#### 2. Experimental work

The small-scale experiments aimed at studying the variability of water elevations and impacts on deck-structures for several wave heights and steepness. Moreover, each test comprised several cycles of regular waves. Although not common for green water evaluation during hull design, the analysis of sequential events was also important for the comparison with the CFD results.

The experimental campaign was conducted at the wave flume of the Department of Naval Architecture and Ocean Engineering of the University of São Paulo, which is 25 m long, 1 m wide and 1 m deep. In the experiments undertaken, the water depth was kept at 0.765m. The wave generation system is comprised of a flap-type wave maker, and the flume presents a passive absorber in the other end, as seen in Fig. 2. Fig. 3 shows the layout and the details of the set-up. The model was placed 11.90m from the wave generator and the length from the generator to the absorber is 18.10m. Wave calibration was carried out at the location indicated in the sketch of Fig. 3 before placing the model in that location. The deviations observed in the calibrated wave parameters were very small (below 3% in wave height and period). Nonetheless, for the analysis presented in the paper, the experimental values obtained in the calibration procedure are always used as a reference for the CFD simulations. Once the model was placed in position, wave transmission across the model was insignificant, and reflections from the wave absorber in the other end of the tank were not a problem. For each one of the tests, the time window for the analysis was defined in order to guarantee that no waves reflected back from the wavemaker and passive absorber could reach the model.

The model was built to represent the cross section of an FPSO hull in a 1:180 scale, see Fig. 4. Two different set-ups were employed, namely with and without a thin plate placed on the side of the hull representing a riser balcony. The balcony was placed 12 mm below the deck (2.16m in prototype scale) and it is 22 mm wide (3.96m in prototype scale). As seen in Fig. 4, the deck is slightly inclined to aid water flowing out of the deck after the green water events.

The wave elevation was monitored by means of four capacitive wave probes in front of the model whereas the forces were measured at the plate over the deck by means of a load cell assembled with a vertical plate, according to Fig. 5, Fig. 6 and Fig. 7.

Wave probe WM01 was located above the deck at a distance of 17 mm from the load cell and WM02 was upstream of the model, respectively at distances of 70 mm and 90 mm from the load cell in the cases without and with the riser balcony. To prevent offset errors in the WM01 readings, a flush mounting cover was attached to the deck surface in the end of wire probe. It is possible to notice

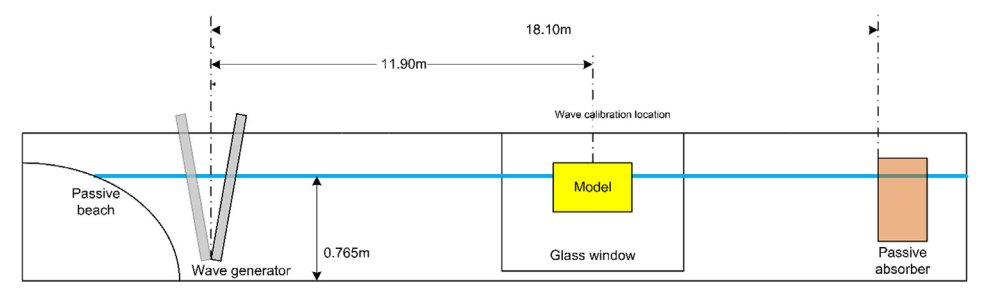


Fig. 3. Sketch showing the experimental setup.

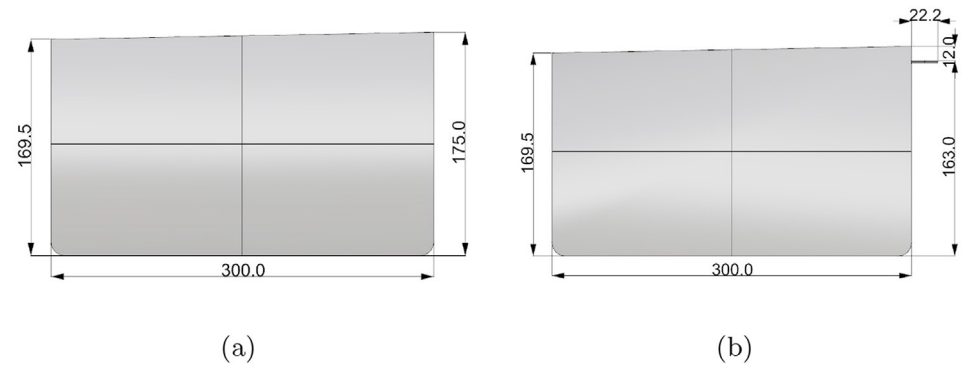


Fig. 4. Cross section of a the FPSO model hull. Dimensions in millimeters. (a) set-up without the riser balcony. (b) set-up with the riser balcony.

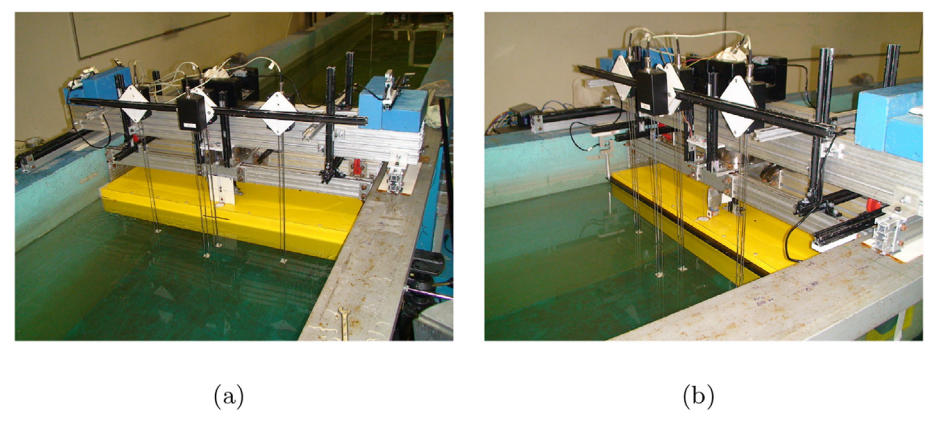


Fig. 5. Model setup. (a) without the riser balcony and (b) with the riser balcony.

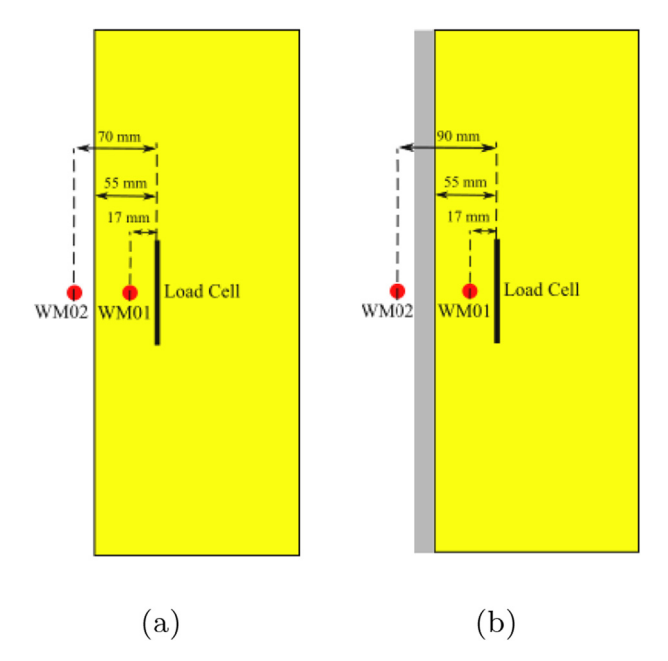


Fig. 6. Top view of model setup without (a) and the riser balcony (b) systems.

the wire and the cover of the probe WM01 in Fig. 7. The impact loads were measured on a small vertical plate measuring  $20 \times 20$  mm assembled at a distance of 55 mm from the hull side (see Fig. 6) and only 3 mm above the deck level. This plate can be seen in Fig. 7, and the reader may notice the red dot in its center. The load cell is connected to this plate and measures the horizontal loads applied



Fig. 7. Picture of the plate assembled with the load cell.

**Table 1** Wave parameters in the model tests and CFD calculations. Scale is 1:180. In this table, T refers to the wave period, H, to the wave height,  $\lambda$ , to wave length and F/A, to the ratio between freeboard and wave amplitude.

Wave ID	Steep. (%)		Model Scale			Prototype		
		T(s)	H (mm)	λ (m)	T(s)	H (m)	λ (m)	F/A
1	4	0.52	17	0.42	7	3.06	76.44	3.65
2	4	0.60	22	0.55	8	3.99	99.84	2.79
3	4	0.67	28	0.70	9	5.05	126.36	2.21
4	4	0.75	35	0.87	10	6.24	156.00	1.79
5	4	0.82	42	1.05	11	7.55	188.76	1.48
6	4	0.89	50	1.25	12	8.99	224.64	1.24
7	4	0.97	59	1.46	13	10.55	263.64	1.06
8	6	0.52	26	0.42	7	4.59	76.44	2.43
9	6	0.60	33	0.55	8	5.99	99.84	1.86
10	6	0.67	42	0.70	9	7.58	126.36	1.47
11	6	0.75	52	0.87	10	9.36	156.00	1.19
12	6	0.82	63	1.05	11	11.33	188.76	0.99
13	6	0.89	75	1.25	12	13.48	224.64	0.83
14	6	0.97	88	1.46	13	15.82	263.64	0.71
15	8	0.52	34	0.42	7	6.12	76.44	1.82
16	8	0.60	44	0.55	8	7.99	99.84	1.40
17	8	0.67	56	0.70	9	10.11	126.36	1.10
18	8	0.75	69	0.87	10	12.48	156.00	0.89
19	8	0.82	84	1.05	11	15.10	188.76	0.74
20	8	0.89	100	1.25	12	17.97	224.64	0.62
21	8	0.97	117	1.46	13	21.09	263.64	0.53

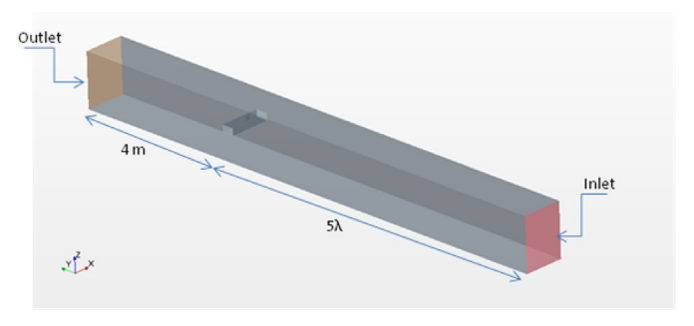


Fig. 8. CFD domain used in the calculations.

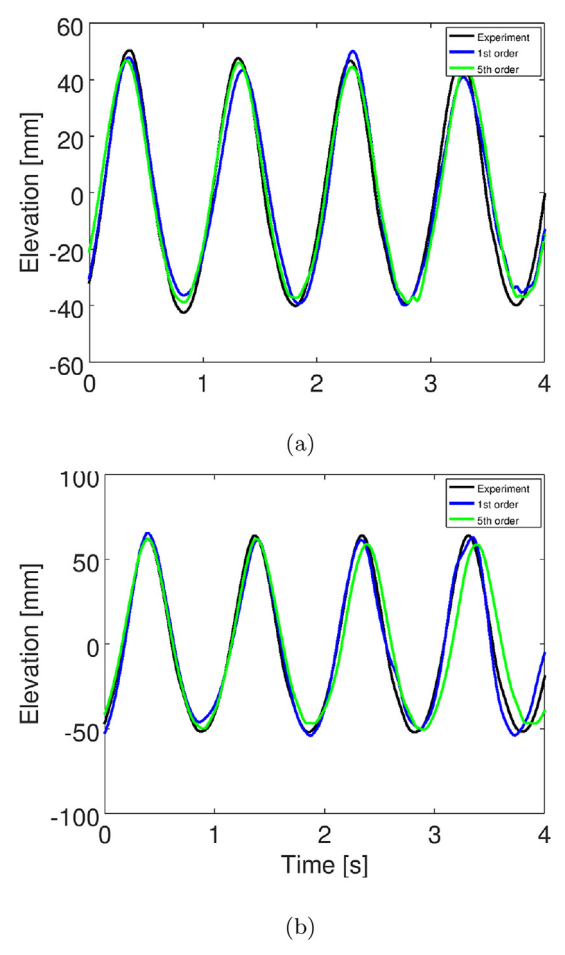


Fig. 9. Wave probe elevation at a distance of 5 wave lengths from the inlet for domain without model hull. (a) Wave Steepness of 6%, T = 0.969s and  $H = 88 \, \text{mm}$  (b) Wave Steepness of 8%, T = 0.969s and  $H = 117 \, \text{mm}$ .

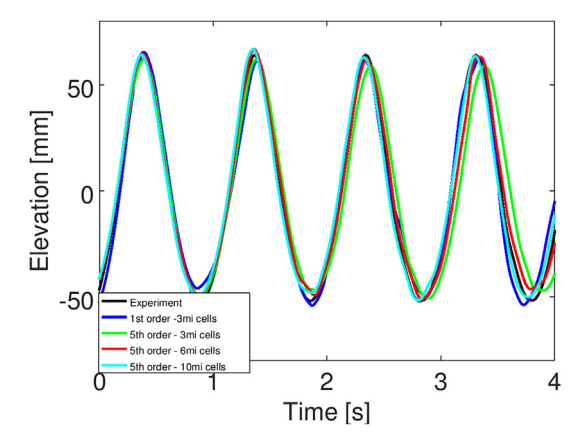


Fig. 10. Wave probe elevation at a distance of 5 wave lengths from the inlet for domain without model hull. Wave Steepness of 8%, T = 0.969s and H = 117 mm.

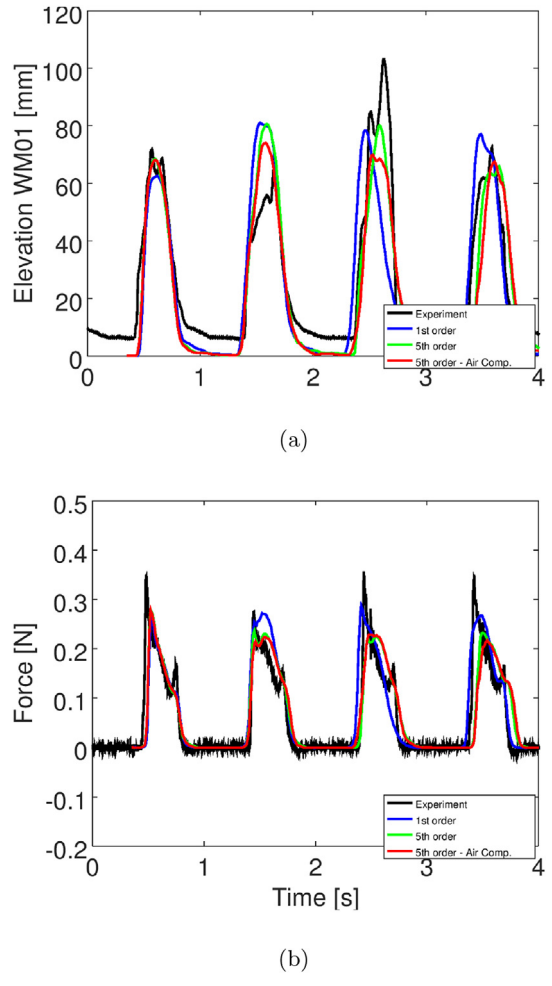


Fig. 11. Wave Steepness of 8%, T = 0.969s and H = 117 mm. (a) Wave elevation WM01. (b) Impact Force.



Fig. 12. Grid layout used in the calculations.

on it. The cell is placed behind the plate and above the deck. An outer plate with overall dimensions of  $100 \times 100$  mm surrounds the small plate. It is not connected to the small plate nor to the load cell, even though its presence deflects the flow and intensifies the hydrodynamic loads. <sup>1</sup>

It should be reminded that the primary purpose of the tests was to provide robust data comprising measurements of wave elevations and loads that would be useful for validating CFD calculations. Accordingly, the vertical plate was not designed with the

<sup>&</sup>lt;sup>1</sup> In fact, it is noticeable that the vertical plate changes the flow compared to a hypothetical situation without it. If the surrounding plate were removed, the measured loads on the cell would be considerably smaller. This aspect also reminds us that the wave impact loads are not independent of the geometry of the deck structures, a fact that still seems to be overlooked by the green water design recommendations currently available.

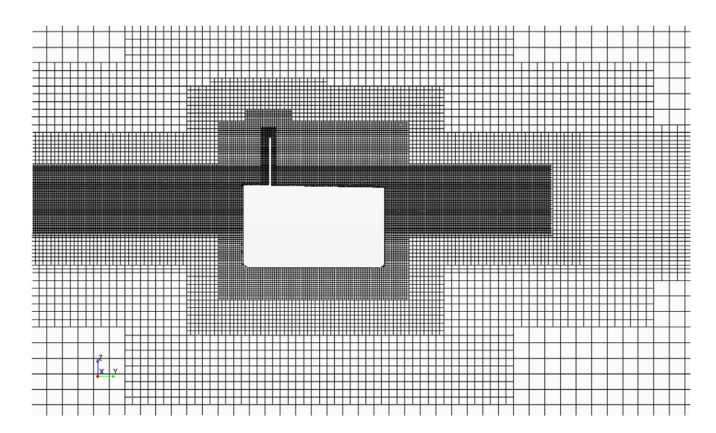


Fig. 13. Details of the grid layout near the hull model.

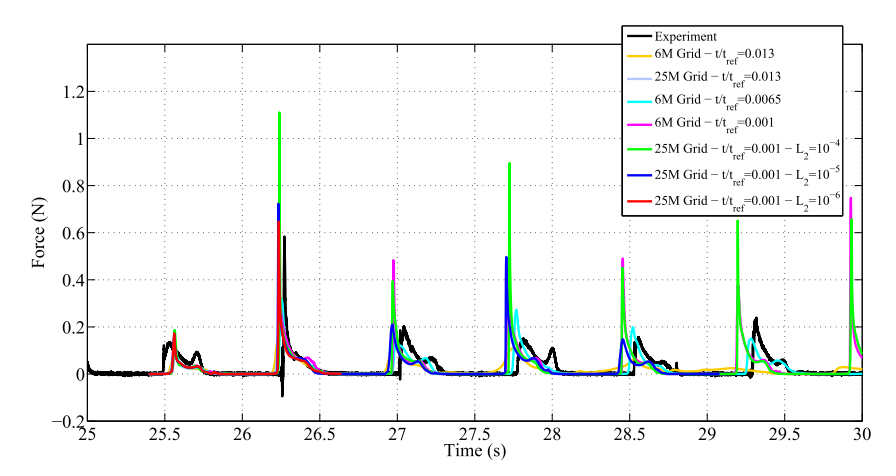


Fig. 14. Discretization and iterative convergence investigation.

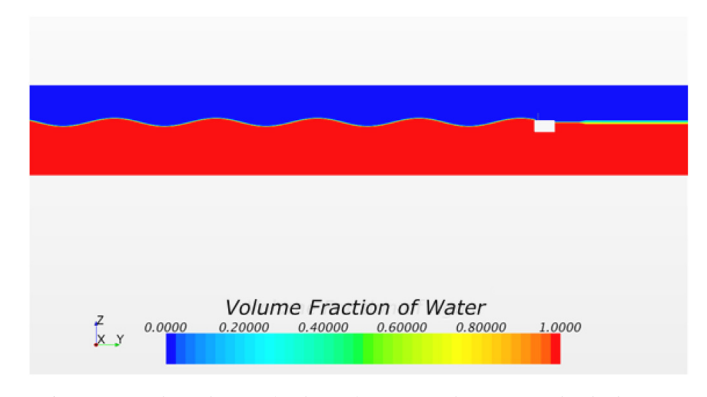


Fig. 15. Initial condition of volume fraction in the numerical calculations.

intention to reproduce any specific deck structure, but instead to make the apparatus stiffer and reduce fluctuations in the load readings (besides protecting the load cell which is placed above deck).

The sampling rate is 300Hz for the wave probes and 4800Hz for the loading cell, which are higher than recommended by International Towing Tank Conference (ITTC) [17].

Finally, Table 1 shows the parameters of the regular waves considered in both the experiments and CFD calculations.

# 3. CFD calculations

The software package StarCCM+ [18] was used for the numerical calculations. The package includes the grid generation, solver

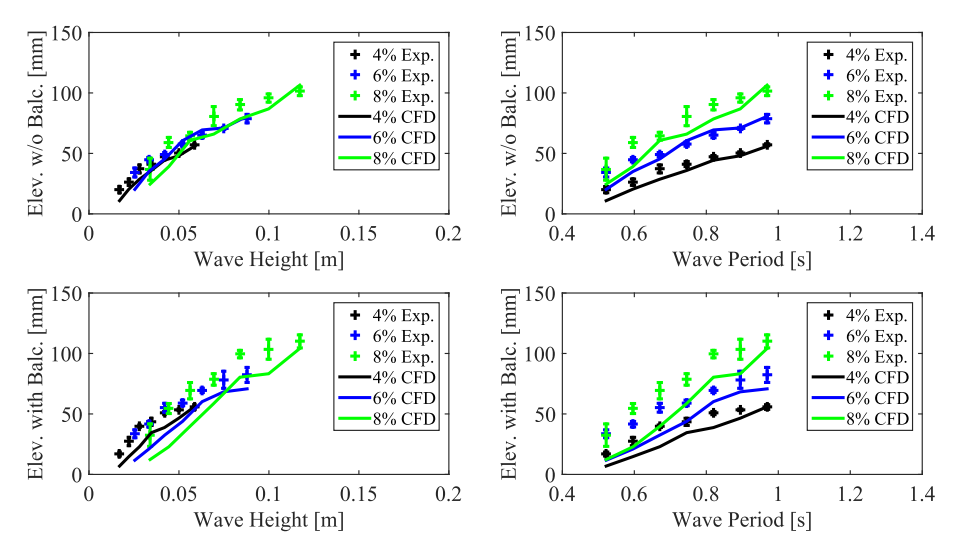


Fig. 16. Mean peak water elevations at WM02 for different incident wave heights and periods without (top frames) and with (bottom frames) the riser balcony.

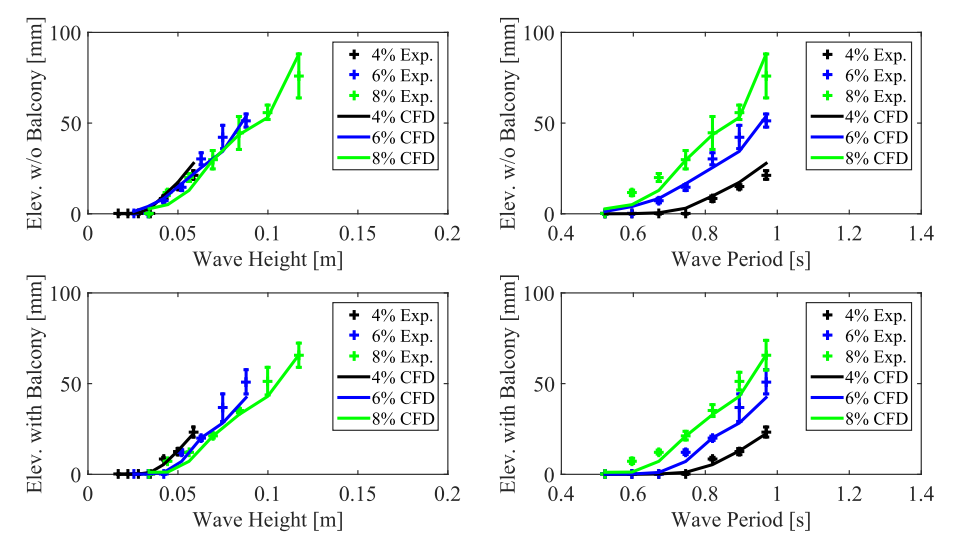


Fig. 17. Mean peak water elevations at WM01 for different incident wave heights and periods without (top frames) and with (bottom frames) the riser balcony.

and post-processing features. It is a collocated, finite-volume based code, which handles incompressible, unsteady, multiphase flows with a VOF-based strategy.

In the present calculations, laminar flow condition has been considered. Furthermore, momentum and pressure equations are solved in a segregated manner, with the reconstruction done based on a Rhie-and-Chow-type pressure-velocity coupling scheme combined with a SIMPLE-type algorithm. Second-order upwind scheme is used for the discretization of convection terms, whereas a second-order central scheme is used for the diffusive flux. A second-order time discretization is also used. For the convection term of the VOF equation, the second-order High-Resolution Interface Capturing (HRIC) scheme is employed. For more details on these schemes, see Ref. [19].

# 3.1. Numerical setup and discretization

Fig. 8 shows the CFD domain modeled for the calculations. The inlet is placed at a minimum distance of 5 wave lengths from the hull centerline, whereas the outlet is  $4 \, \text{m}$  away from the model and the domain width is  $1 \, \text{m}$ . The water depth is  $0.765 \, \text{m}$  and the height above the mean water level is  $0.5 \, \text{m}$ .

Regarding the boundary conditions, at the inlet a velocity inflow applies, whereas at the outflow, an outflow pressure boundary condition holds. A wall boundary condition is used on the sides and bottom and a pressure boundary condition is applied on the top

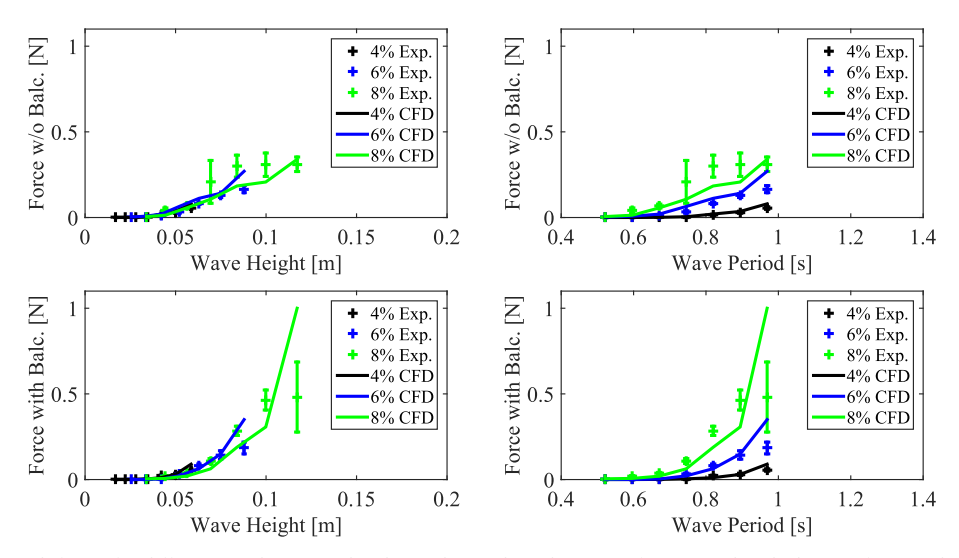


Fig. 18. Mean peak forces for different incident wave heights and periods without (top frames) and with (bottom frames) the riser balcony.

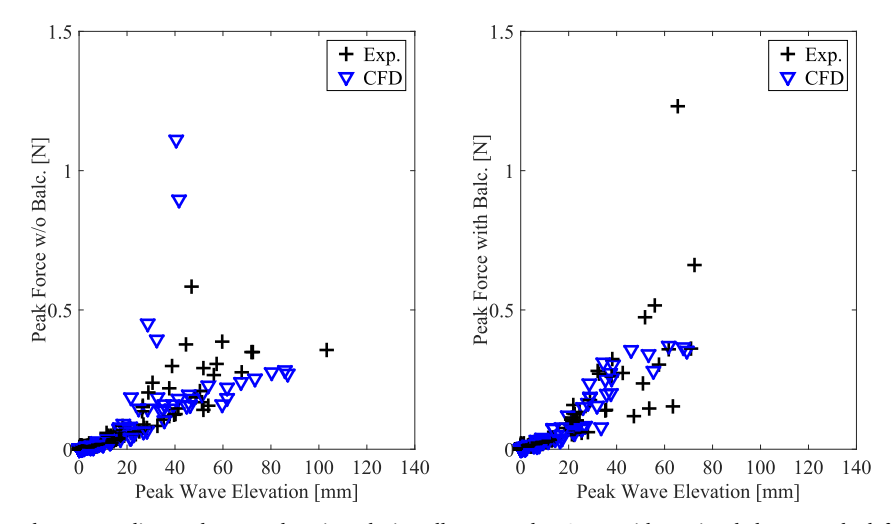


Fig. 19. Peak forces and corresponding peak water elevations during all wave cycles. Setup without riser balcony on the left and setup with riser balcony on the right.

# boundary.

The waves are prescribed in the inflow boundary as linear (first order), despite the fact that some of them are quite steep (up to 8%). In fact, it would be reasonable to expect that, for the steepest waves, nonlinear effects would start to have an influence on water entry and wave impact. Nonetheless, previous analysis done with the steepest waves and the 5th order Stokes wave model has not confirmed these expectations. In order to illustrate this point, a few results concerning the agreement on the wave profile recorded on the wave calibration tests (measured in the flume without the hull model) are presented in Fig. 9. For these waves, the steepness is 6% (a) and 8% (b), and both CFD wave models (1st and Stokes 5th order) were run with the same iterative convergence levels, time and space discretization (in this case, a 3 million cells grid). One may notice that, for the 6% steepness wave, the agreement of the different inflow wave conditions is practically equivalent, while for the 8% steepness wave the nonlinear wave model seems to be more susceptible to numerical dissipation. In fact, the effects of numerical dissipation can be attenuated with a more refined grid. This is attested by the results of Fig. 10, in which the same conditions of Fig. 9 (b) are reproduced with finer grids (up to 10 million cells). It becomes clear that the agreement of amplitudes and periods of the 5th order waves improve with grid refinement, but it is not possible to conclude that they do provide a better representation of the physical wave, if compared to the results of the linear wave model. Additional simulations have been made for measuring the effects of the 5th order model on the wave impact loads for some of the steepest wave tests. Fig. 11 shows the wave elevation on the hull side and subsequent impact loads for some of the waves with 8% wave steepness, including the 5th order model and also simulations with nonlinear waves and air compressibility. Again, given that no visible improvement of the results was attained with the nonlinear wave model and air compressibility, the first order model was employed throughout the analyses for the sake of saving computational time and effort. As a final remark in this regard, it seems reasonable to speculate that the observed insensibility to the wave model may be linked to the high ratios of wave amplitude to

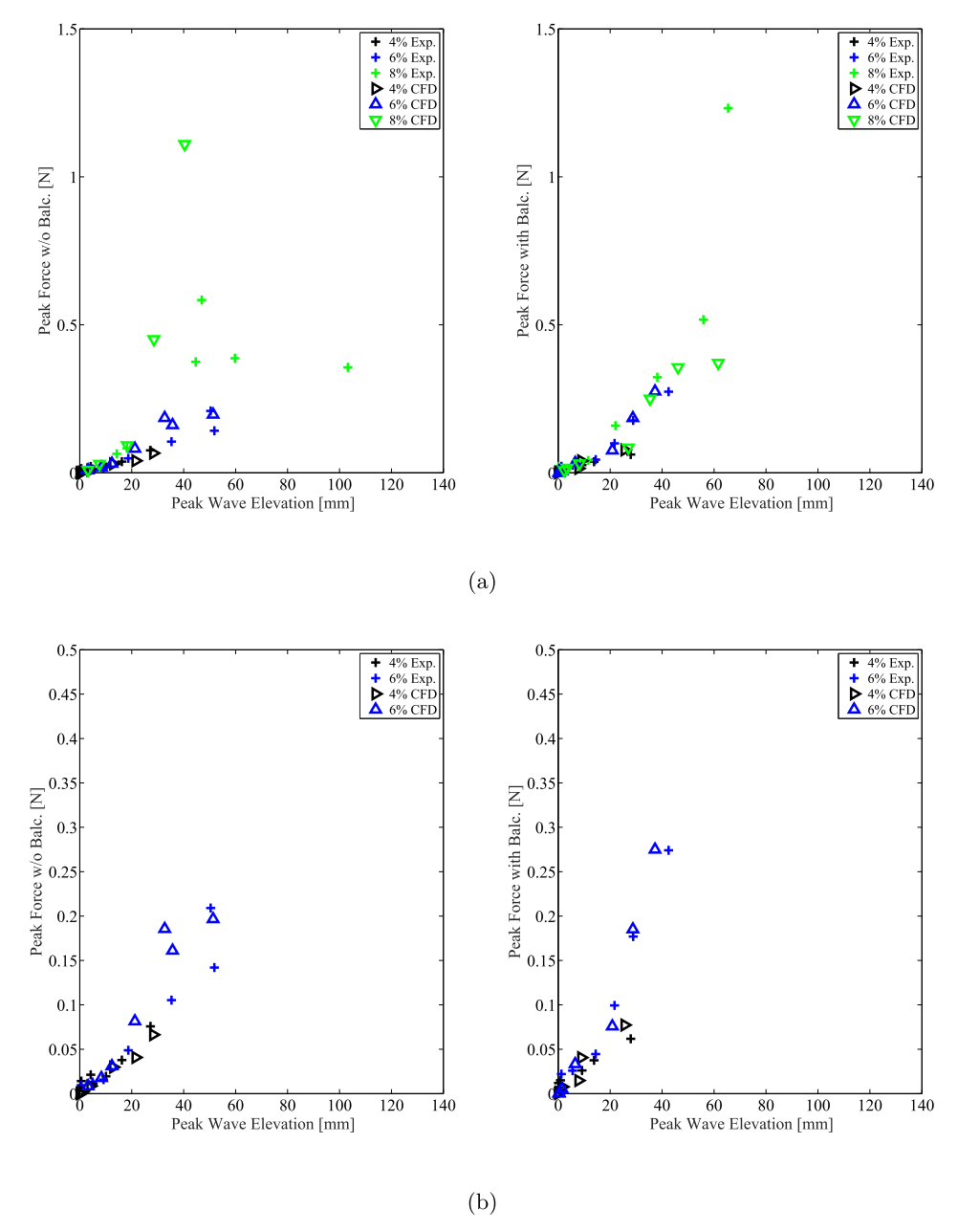


Fig. 20. Maximum peak forces and corresponding peak water elevation at each realization. Setup without riser balcony on the left and setup with riser balcony on the right. (a) All steepness. (b) 4% and 6% steepness.

freeboard and, consequently, to the massive water flows on deck in these particular tests. It is possible (although not confirmed in the present study) that steep waves facing a higher freeboard (when wave run-up effects are more pronounced) would be more intensively affected by the nonlinearities of the incoming waves.

Due to the large number of simulations and the long runs necessary to achieve nearly steady-state conditions, discretization and iterative convergence analyses were carried out based on the case with wave height of 69 mm and wave period of 0.75s (Wave ID 18, see Table 1). In this investigation, time steps were varied from 77 steps to 1000 steps per wave cycle, iterative convergence criteria based on the r.m.s. norm ( $L_2$ ) of all variables dropping from  $10^{-3}$  to  $10^{-6}$  and the number of grid cells from 6M to 25M cells. The grids are based on a grid layout and the variation of a base-size is done in order to obtain grids as geometrically similar as possible.

Fig. 12 shows the grid layout for the calculations. The grids are unstructured hexahedral with five refinement blocks, from which three blocks contain the free surface and two blocks contain the hull model. The finest free-surface refinement block extends from the inlet to the hull model, being less refined downstream of the hull. All the refinement blocks have their parameters related to a base size which is adjusted for each test to obtain at least 80 cells per wave length and 20 cells per wave height. Fig. 13 shows the grid

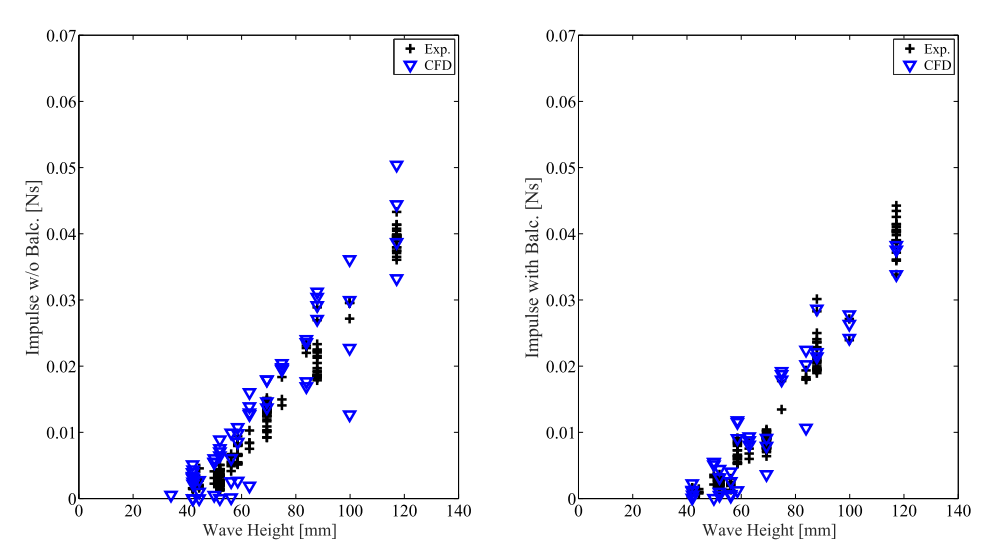


Fig. 21. Impulse values and corresponding peak water elevations. Setup without riser balcony on the left and setup with riser balcony on the right.

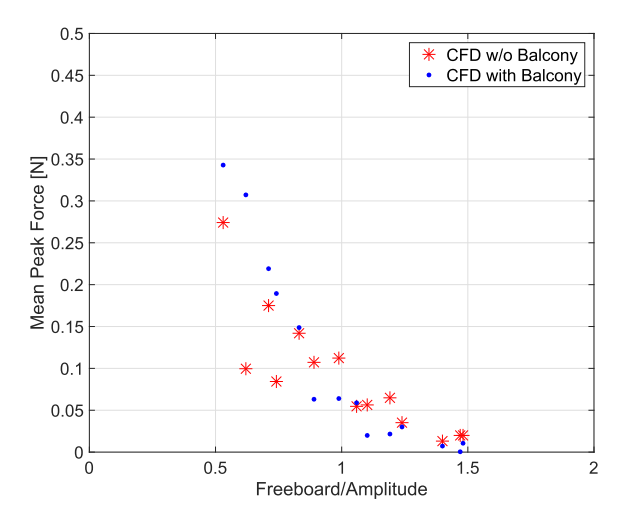


Fig. 22. Mean peak forces and corresponding freeboard-to-amplitude ratios for the CFD results.

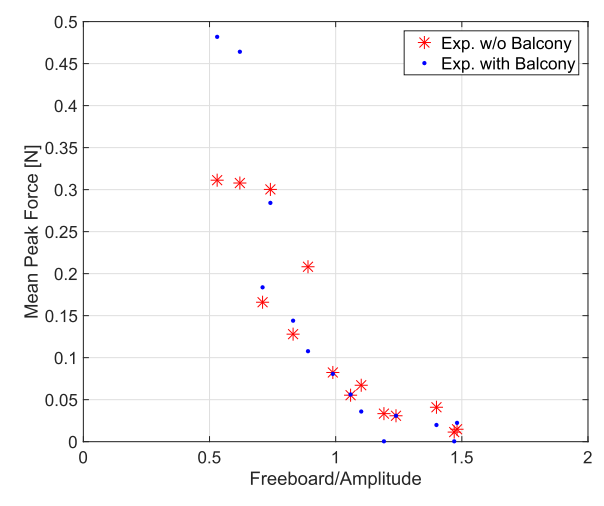


Fig. 23. Mean peak forces and corresponding freeboard-to-amplitude ratios for the experimental results.

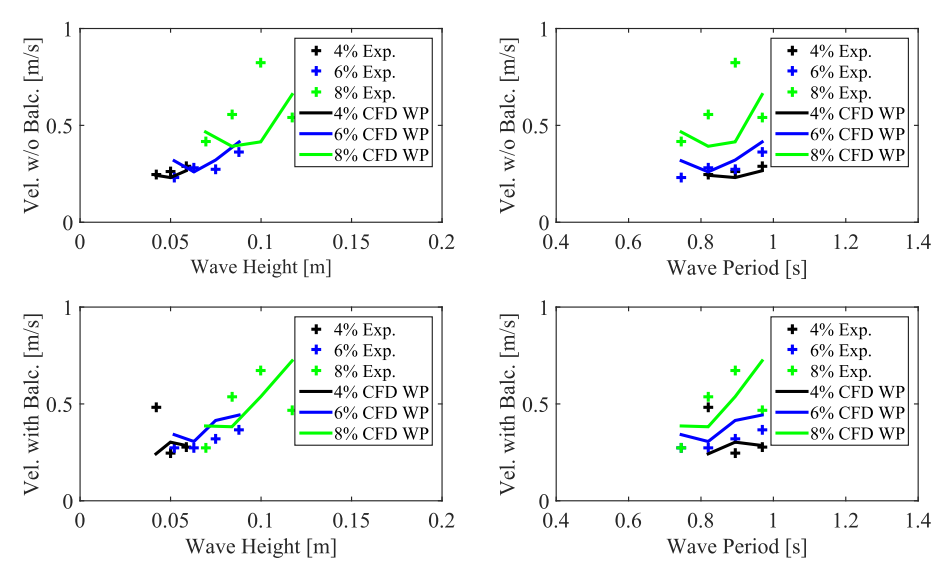


Fig. 24. Water velocity above the deck (measured by means of the probes WM01 and WM02) from the experiments and CFD calculations.

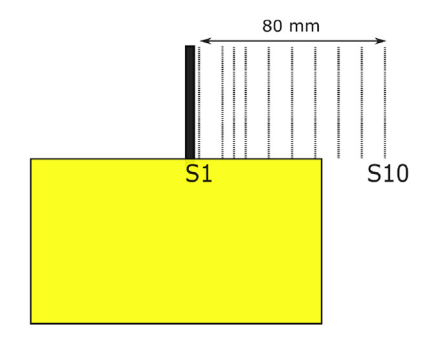


Fig. 25. Positions of the stations where the fluid velocity is measured above the deck and the distance between the wave probes.

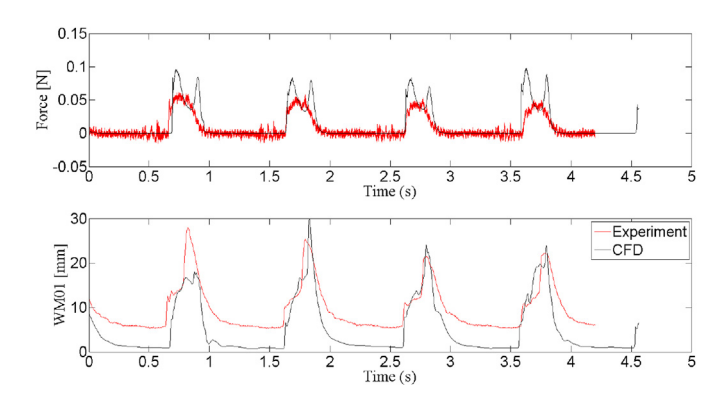


Fig. 26. Time traces of force (upper fig) and wave elevation (lower fig) for the case with wave height 58 mm and period 0.97s. Set-up with riser balcony.

## details near the hull model.

In order to illustrate the effects of the discretization, Fig. 14 presents a comparison of the numerical predictions of impact forces on the load cell and the experimental measurements for the tests with wave ID 18 (without the riser balcony). This plot shows the time traces of forces at the load cells for each setup, combining time steps, grids and iterative convergence criteria. One may realize that there is no clear trend with regards to these parameters, meaning that more refined grids and time steps do not lead to a consistent trend in peak force variation. Similarly, the adoption of different iterative convergence criteria does not seem to guarantee a consistent trend. From a practical standpoint, the conclusion is that the peak forces are so nonlinear and sensitive to the discretization and iterative errors that probably higher order schemes and much lower iterative errors ought to be achieved for a sound

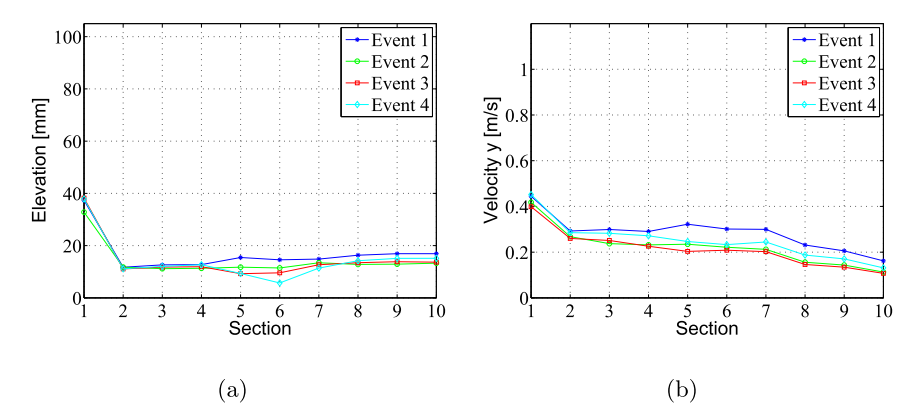


Fig. 27. Elevations (a) and Water horizontal mean velocity (b) at the moment of peak force for the case with wave height 58 mm, period 0.97 s at each of the ten stations. Set-up with riser balcony.

conclusion. Moreover, the stochastic nature of the force peaks together with the short duration of the events would require both very small time steps and large number of events to support such conclusion. The variations obtained with the 6M cells grids (and larger),  $t_{ref}/t > 154$  ( $t_{ref}$  is the wave period and t is the time-step) and  $L_2 < 10^{-3}$  seem random due to the nature of the phenomenon.

Evidently, one should aim at the most refined discretization and more strict iterative convergence criteria; however, a compromise between hardware usage, computation time and accuracy was enforced, and for this reason the parameters above were adopted for all calculations. Therefore, for all tests, the grids present 80 cells per wave length and 20 cells per wave height, whereas the time steps are chosen so that 154 steps are calculated in each wave cycle. Finally, the adopted iterative convergence criteria is  $L_2 < 10^{-3}$  for all variables.

The initial conditions are imposed in the domain according to the linear regular wave fields (velocity, pressure and volume fraction), as presented in Fig. 15.

#### 4. Overview of experimental and numerical results

This section presents a comparison between the experimental measurements and numerical predictions. Part of this comparison can be done directly on the time records, and this is the case for the wave elevation in the different probes and the impact force. However, the analysis is complemented by the computation of some other quantities, which are important regarding the green water phenomenon, such as the force impulse (obtained from time integration of the force signals when the water elevation exceeds the freeboard) and an estimate of fluid velocity above the deck. The latter was not measured in the experiments, so the estimates are made indirectly, based on the signal phase between in-line wave probes.

#### 4.1. Water elevation results

Fig. 16 presents the mean values of maximum (peak) water elevation at the WM02 wave probe. Results for different wave steepness are presented, namely 4%, 6% and 8%, as function of both incident wave heights and wave periods. The upper figures correspond to the tests and simulations with the bare hull and the lower ones present the results for the same wave conditions when the riser balcony was attached to the hull model. Both numerical predictions and experimental results are presented, and the experimental results present vertical bars that denote the standard deviation of the peak elevations in each test. These bars thus provide a measure of the variation of the peak elevation for the different wave cycles in each test. In each case, at least 10 wave cycles with nearly steady state conditions were considered in the experiments. Regarding the numerical analysis, the initial condition already represents the regular wave front at the hull side, as previously shown in Fig. 15. For this reason, the simulations were made for no less than 5 wave cycles, and the first one was discarded in the analysis. It should be noticed that the CFD results also present a variation of peaks for the different cycles (as can be seen, for instance, in Fig. 14. The standard deviations of the numerical predictions, however, are not depicted in the same figures for the sake of clarity of the results. Moreover, also with the purpose of an easier visualization, the CFD results for the same steepness are depicted in continuous lines, although the simulations were made only for the same conditions of the experiments.

From the results in Fig. 16, one may realize that there is an increase in the mean values of peak elevations both with wave heights and periods. However, when observed against the wave periods, the effects of the wave steepness can be seen more clearly. Finally, the presence of the riser balcony does not seem to induce significant changes in the experimental wave elevations, although, especially for the largest wave steepness (8%), it does increase the discrepancies regarding CFD results.

Fig. 17 shows the mean values of peak water elevations for the wave probe WM01, which is placed above the model deck. It indicates, therefore, the amount of water that actually embarked on deck in each test. The trends are similar to the ones observed for the WM02 location, although in this case the agreement of experimental and CFD results is better, especially for the steepest wave, which is somewhat unexpected.

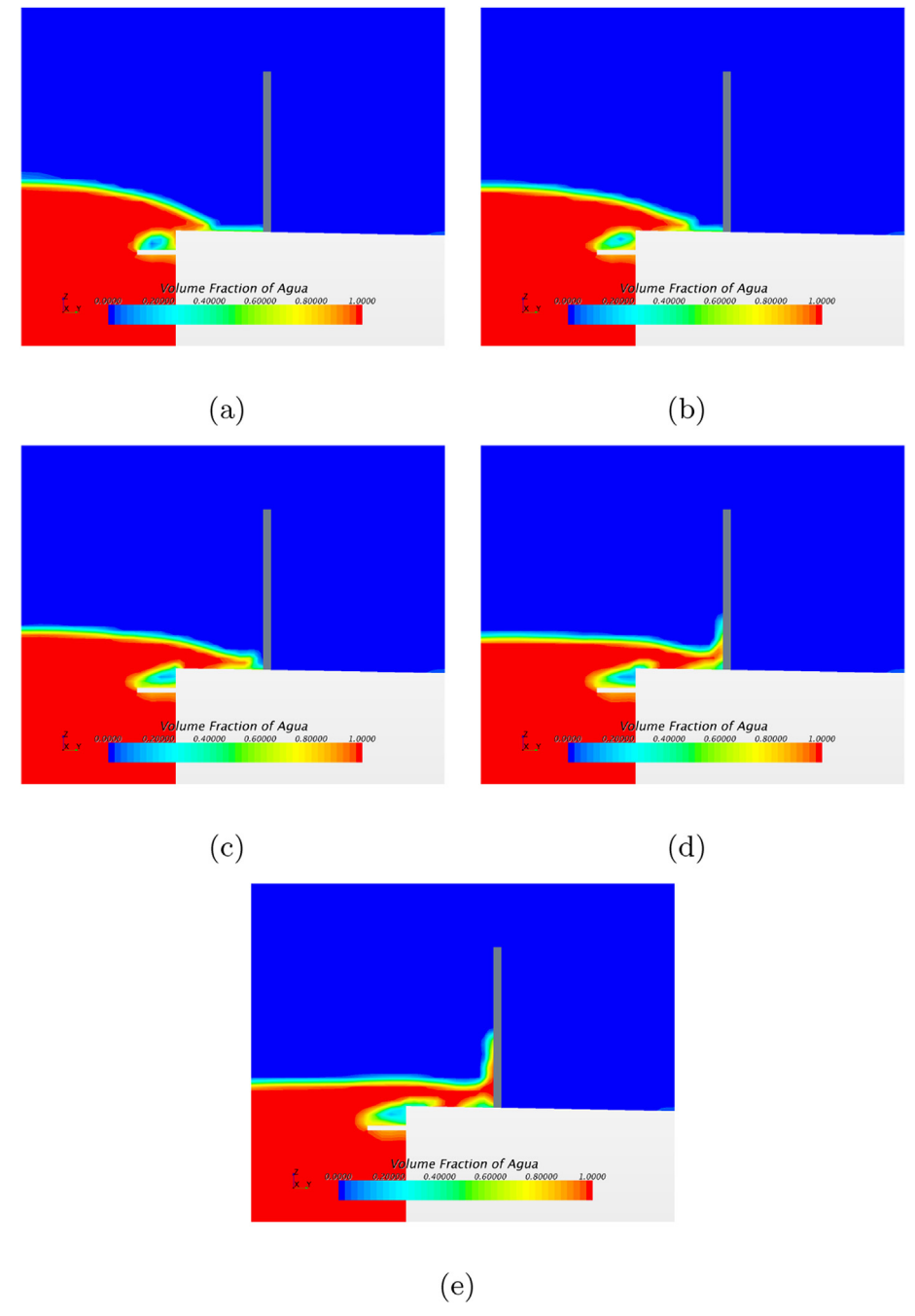


**Fig. 28.** Frames showing volume fraction distribution with the evolution of the water for the first peak. (a)  $t_{peak} - t = 0.08s$ . (a)  $t_{peak} - t = 0.08s$ . (b)  $t_{peak} - t = 0.04s$ . (c)  $t_{peak} - t = 0.02s$ . (e)  $t_{peak}$ . Setup with riser balcony.

# 4.2. Force impact results

Fig. 18 presents mean values of maximum (peak) force measured on the 20 mm x 20 mm load cell. The pattern for the presentation remains the same: top and bottom figures present the results with and without the riser balcony, respectively. Once again, the force results are plotted against incident wave heights and periods. For each test, the standard deviations of the measured peak forces in different wave cycles are presented as vertical bars. One may notice that there is fair agreement between experimental and numerical results regarding trends and values, except for the waves with steepness of 8%. The riser balcony does not induce a clear and consistent trend in mitigating the impact forces and, for waves with steepness of 8%, the impact forces are sometimes larger in the set-up with the balcony than without it. Interestingly, on the left frames there is small variation in the average peak forces from

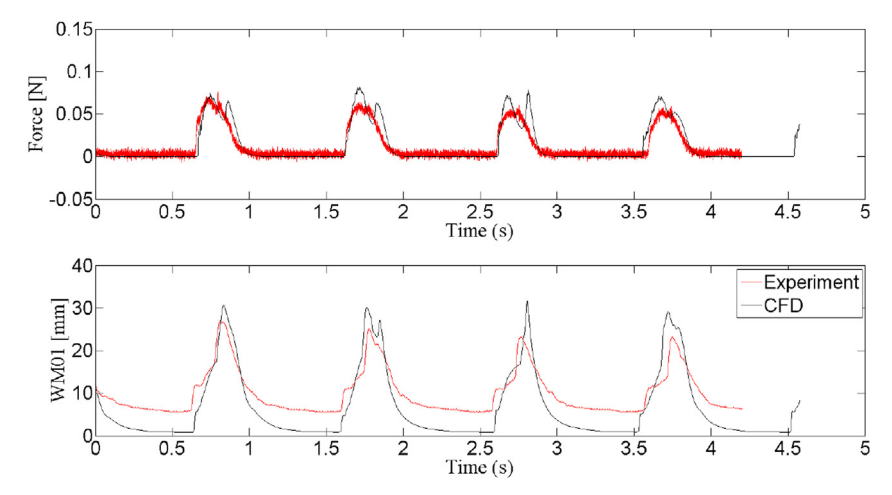


Fig. 29. Time traces of force (upper fig) and wave elevation (lower fig) for the case with wave height 58 mm and period 0.97s. Set-up without riser balcony.

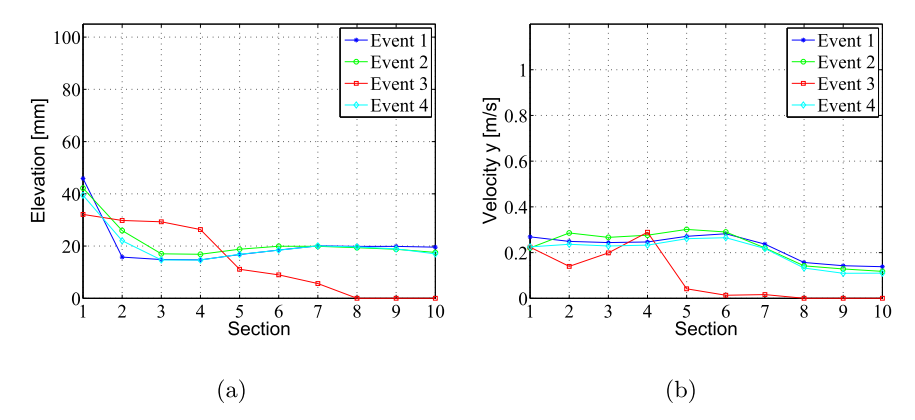


Fig. 30. Elevations (a) and Water horizontal mean velocity (b) at the moment of peak force for the case with wave height 58 mm, period 0.969 s at each of the ten stations. Setup without riser balcony.

different wave steepness, except for the experimental values of 8% waves. That is in agreement with the elevation results presented above. For the more steep and nonlinear waves, one should notice that not only the average force values are larger, but also the standard deviation of the measured peaks in each test. When large amounts of water move upon the deck, the variations from cycle to cycle become more pronounced.

In Fig. 19, the peak forces are plotted against the corresponding maximum (peak) water elevations for the same water shipping events (measured at the hull side, in WM02). The set-up without balcony shows larger scatter for the CFD results than for the experimental ones, while the opposite occurs for the set-up with the riser balcony. For low peak forces and elevations, the results display an almost linear relation up to approximately 30 mm peak elevation, both with and without the balcony. Conversely, for higher peak elevations and forces, a higher scatter is noticed.

In Fig. 20, the maximum force at each run is plotted against the corresponding peak water elevation. Numerical and experimental results for both set-ups show fair agreement, except for the 8% steepness waves, particularly for the largest water elevations. For those cases, the CFD results show larger force amplitudes than for the experiments whereas, for the set-up with the balcony, the experimental results show larger amplitudes. There is no coherent trend comparing the set-ups with and without the balcony. Evidently, since the larger waves have amplitudes which are much higher than the freeboard, one should not expect relevant mitigation of the force impacts by the riser balcony in this case.

Regarding the forces, an additional analysis can be made. Instead of observing only the force peaks, which are more sensitive and prone to variations both in the experiments and numerical simulations, a comparison can be made based on the force impulse. The impulse corresponds to the integration of the force in time. The time span considered for computing the force impulse corresponded to the interval during which the wave exceeded the freeboard level, according to the readings of the wave probe located on the hull side (WM02). Fig. 21 shows the impulse values and the corresponding incident wave height for the cases with and without riser balcony for each run. Naturally, as an integral quantity, the impulse values tend to correlate more linearly with the incident wave heights than the peak forces, mitigating part of the fluctuations that are inherent when dealing with the peaks. In spite of that, there is still some spread in the data. No significant differences can be seen with the presence of the riser balcony, again showing that this

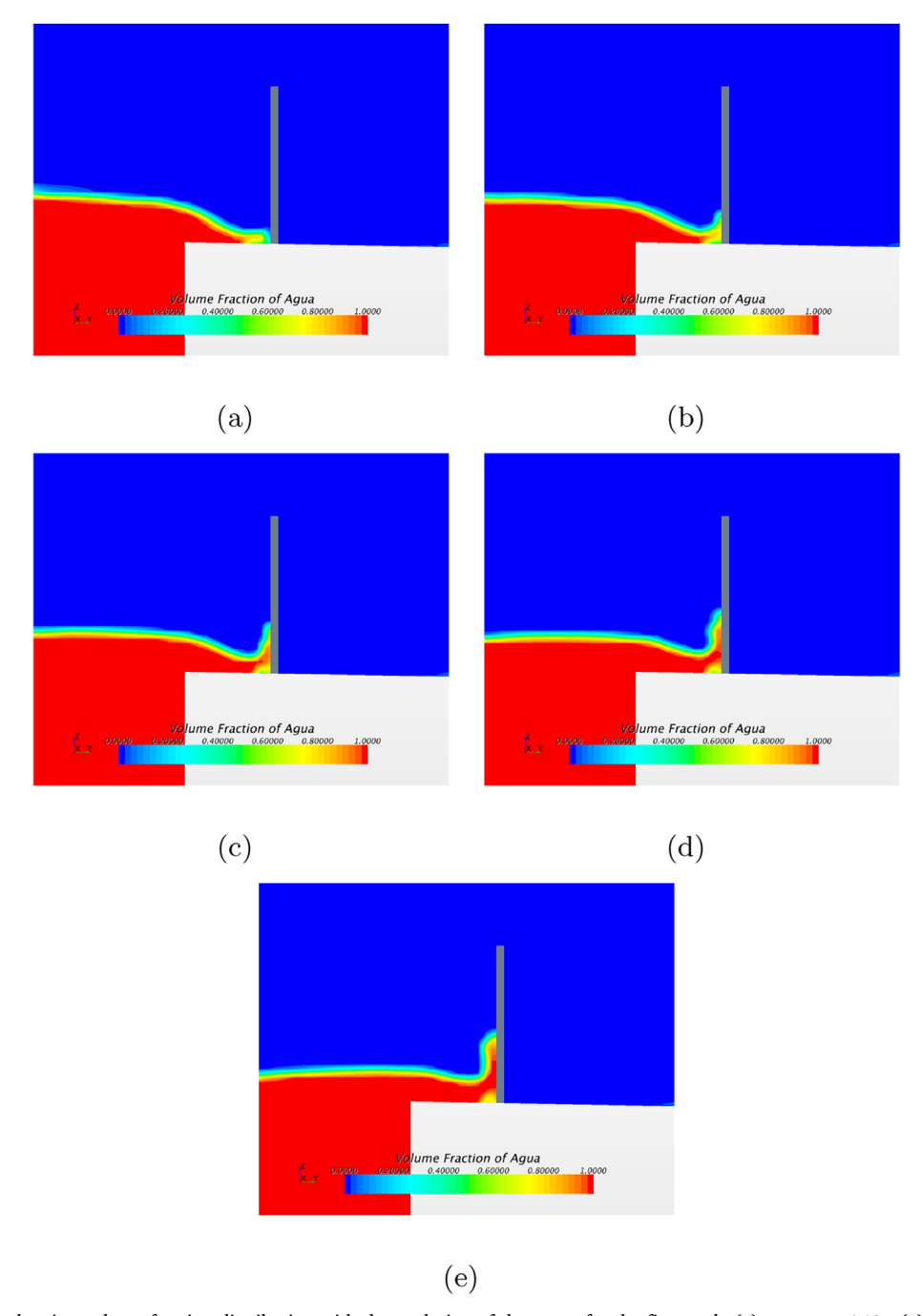


Fig. 31. Frames showing volume fraction distribution with the evolution of the water for the first peak. (a)  $t_{peak} - t = 0.08s$ . (a)  $t_{peak} - t = 0.08s$ . (b)  $t_{peak} - t = 0.04s$ . (c)  $t_{peak} - t = 0.02s$ . (e)  $t_{peak}$ . Setup without riser balcony.

particular device does not have a relevant impact for the wave conditions that were tested. Interaction of the waves with flow from previous wave cycles seems to have a high relevance, being the probable cause of the observed spreading in the data. Nonetheless, it is important to remark that the agreement between the impulses predicted from the tests and corresponding CFD simulations is good. This is very important for the purpose of subsequent structural analysis. This analysis is often done based on equivalent static forces, and the criterion for defining these equivalent forces is still a subject of dispute. It is usually accepted that, if based purely on the impact peaks, the uncertainties will be high and the equivalent forces too conservative. The good estimations regarding the impulses, on the other hand, at least add some predictability to this very complex problem.

In order to visualize the influence of the balcony on the mean peak forces in the present results, Figs. 22 and 23 show the mean peak forces against freeboard-to-amplitude ratio, respectively for the calculations and for the experiments. The freeboard-to-

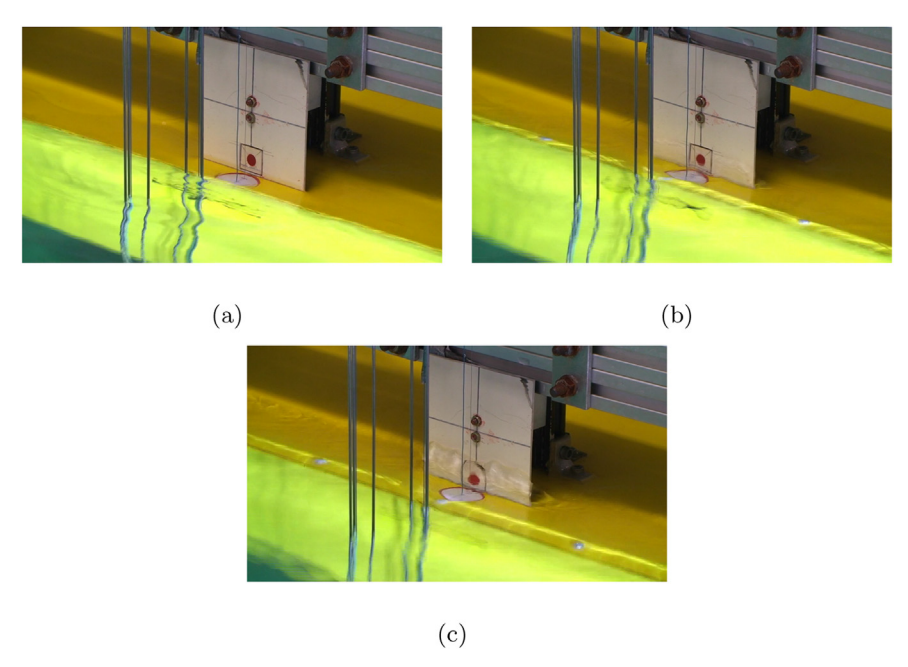


Fig. 32. Example of dam-break type event from the experiments.

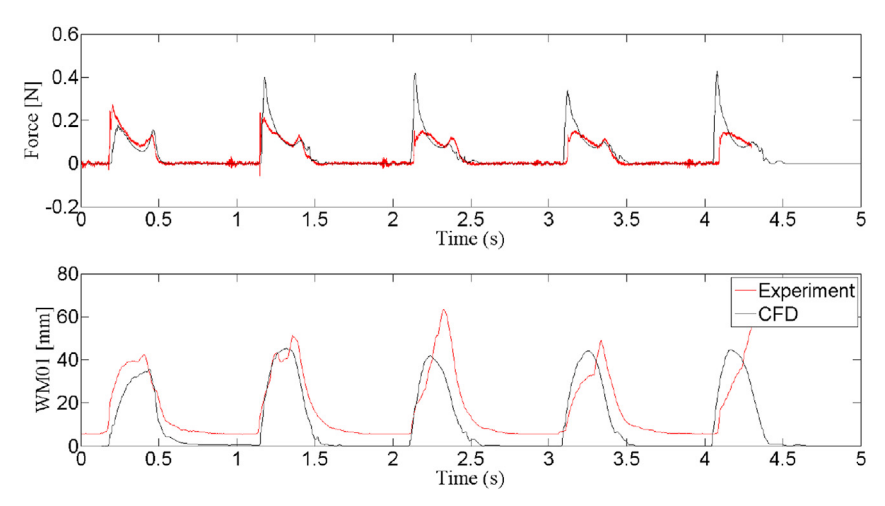


Fig. 33. Time traces of force (upper fig) and wave elevation (lower fig) for the case with wave height 88 mm, period 0.97s. Set-up with riser balcony.

amplitude ranges from 0.5 to 1.5 for the cases with and without the balcony. Both numerical and experimental results show no clear pattern comparing the cases with and without the balcony. However, the CFD results with the balcony seem to indicate a trend of reducing the impact forces for the higher freeboard-to-amplitude ratios and an opposite effect for the lower values of this ratio.

# 4.3. Water velocity results

Another measurement that may be considered interesting concerns the velocity of propagation of the water front on the deck. No direct measurement of velocity was made in the tests, but an attempt can be make by estimating it based on the distance between probes WM01 and WM02 and the time elapsed between the passage of the wave peak at the location of these probes. The estimated velocities can then be compared to those obtained from the numerical simulations. The results are summarized in Fig. 24, which presents the comparison of the water front velocity above the deck calculated from the experimental and numerical results. Clearly, the agreement between CFD and experimental results is poor, indicating both some randomness of the phenomena and, in some extent, the inaccuracy of this method. The water velocity increases with increasing wave steepness, but not without important scatter. Once again, wave periods seem to induce larger scatter of the water velocities above the deck. A more thorough investigation on the variation of the front velocity will be presented ahead.

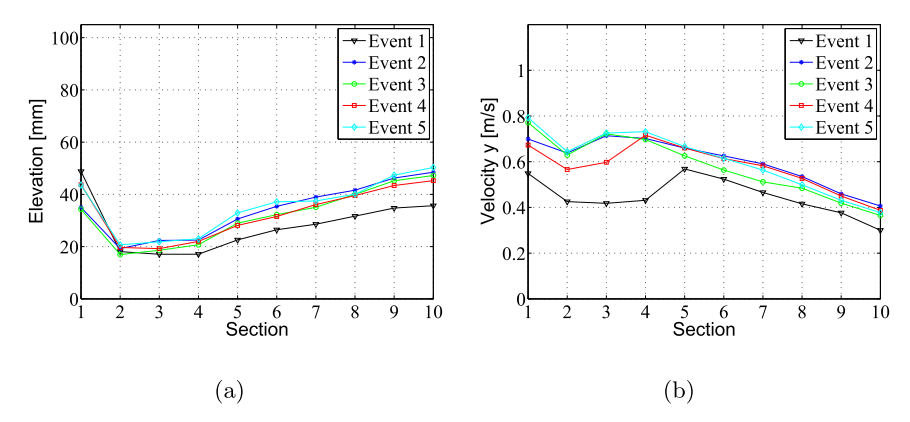


Fig. 34. Elevations (a) and Water horizontal mean velocity (b) at the moment of peak force for the case with wave height 88 mm, period 0.97 s at each of the ten stations. Setup with riser balcony.

## 5. Detailed analysis of selected cases

In this section, a deeper investigation is done on the behavior of water shipping for three cases with period of 0.97s and wave steepness of 4% (wave height of 58 mm and freeboard-wave amplitude ratio of 1.06), 6% (wave height of 88 mm and freeboard-wave amplitude ratio of 0.71) and 8% (wave height of 117 mm and freeboard-wave amplitude ratio of 0.53). The simulated set-up is the same as presented above, with and without the riser balcony. The main objective of this study is to investigate how the variability observed on the impact forces correlates to water elevations, evolution of the water on deck profile and flow velocities. The wave conditions were selected based on this objective, since these waves were the ones that produced the largest water shipping events and variability for each wave steepness.

In all cases, the forces are measured at the load cell and water elevation is presented at the wave probe WM01. The following sections show the distributions of water elevations, forces and velocities in each condition. The velocity measurements are based on the CFD simulations are done in ten locations (probes), 7 on the deck and 3 outside, S1 to S10. The probe S1 is at the face of the plate and the others are placed 10 mm apart from each other, except for S3, which is 5 mm away from S2 and S4.

#### 5.1. Wave steepness 4%

# 5.1.1. Case with riser balcony

Fig. 26 shows force and water elevations time traces (measured at WM01) for the case with wave height of 58 mm and period of 0.97s. The maximum values of wave elevations are generally well reproduced in the CFD simulations, except for some water that remains on the deck after each water shipping event in the experiment (in the CFD calculations, the water leaves the deck as there is a perfectly plane and smooth surface). There is also reasonable repeatability in the different cycles. The impacts in this case are not severe, so the loads are relatively small. Although the match in wave elevations is good, one may realize that the CFD computations tend to overestimate the forces measured in the tests. In addition, the shape of the force cycle with two peaks is not observed in the signal obtained from the load cell. The absence of the second peak is probably related to the fact that the level of water that remains on the deck between two consecutive water shipping events is larger than the one predicted by the CFD simulations.

Based on the CFD results, Fig. 27(a) and (b) present the water elevation and horizontal velocity on the deck at the moment of peak force along the ten probes and for each one of the 4 impact events. The velocity was calculated as the area-averaged fluid velocity on a  $20 \times 20$  mm square at each of the 10 sections in Fig. 25. There is reasonably small height and velocity variation along the ten probes, with the maximum values at S1 (in front of the plate). In this case, it seems that due to the larger amount of water reaching the deck, relative to the case with smallest incident-wave steepness, the slamming and rise-up phenomena are more defined in the simulation, which also show the general presence of two peaks in the force.

In Ref. [10], mainly two water-on-deck profiles with subsequent impact are identified, namely the one with water plunging directly against the structure on deck and the one that resembles a dam break profile. The latter is identified as the most common green-water event, which tends to cause lower impact loads forces than the plunging-type events.

For characterizing the type of green water events in this case, Fig. 28 shows the progress of the water for the first event by means of the volume fraction distribution at different time steps. The last frame corresponds to the moment of the force peak. In spite of the presence of the riser balcony, there is a large portion of water that enters the deck causing an impact that resembles the dam-break type. Air entrapment due to the presence of the riser balcony is also clear.

<sup>&</sup>lt;sup>2</sup> Unfortunately, there was no available equipment capable of capturing the images of the flow evolution with sufficient accuracy during the tests in the wave flume. For this reason, the analysis of the water on deck progression is based exclusively on the simulations.

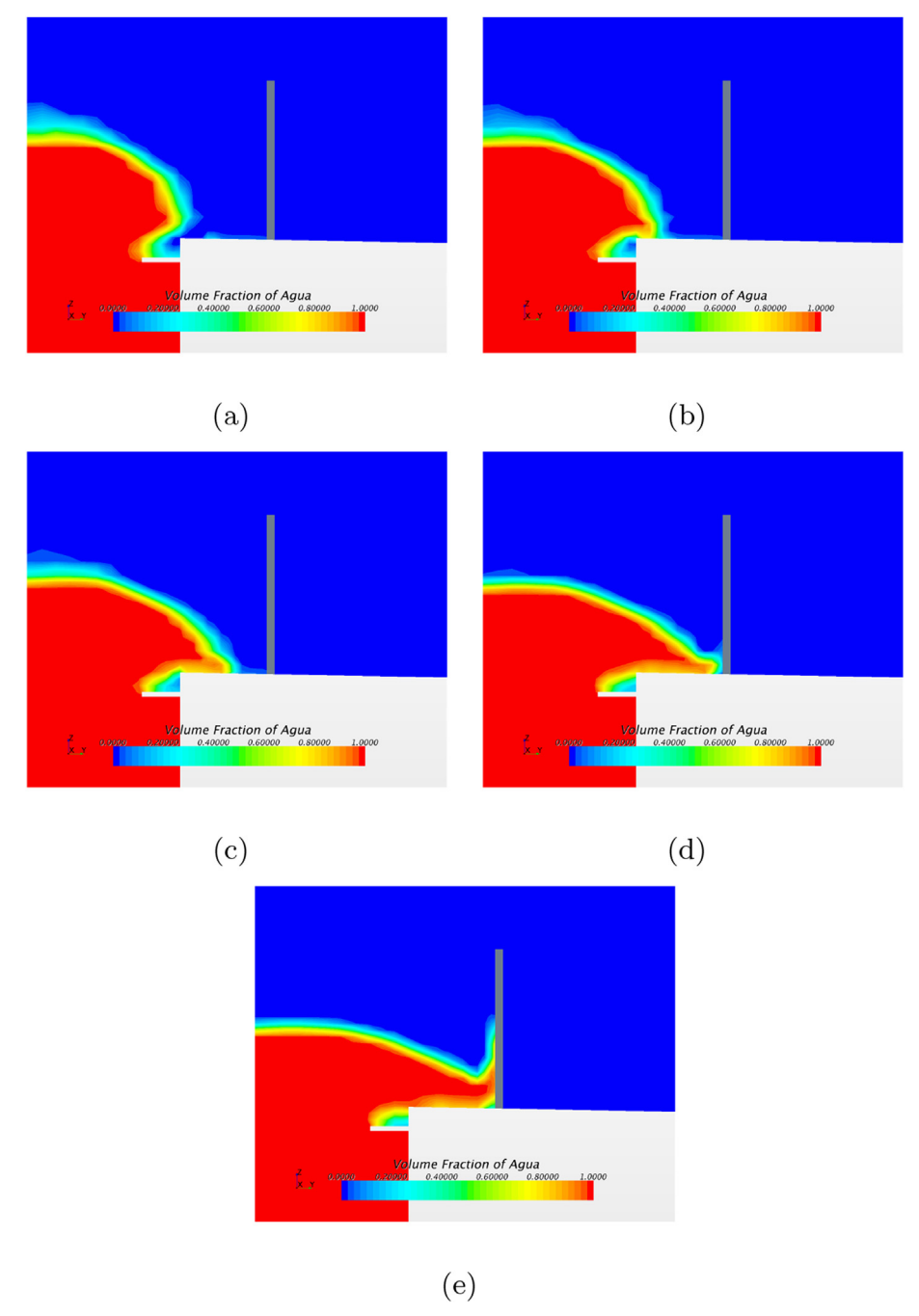


Fig. 35. Frames showing volume fraction distribution with the evolution of the water for the fourth peak. (a) $t_{peak} - t = 0.08s$ . (a) $t_{peak} - t = 0.08s$ . (b) $t_{peak} - t = 0.04s$ . (c) $t_{peak} - t = 0.02s$ . (e) $t_{peak}$ . Setup with riser balcony.

# 5.1.2. Case without riser balcony

Fig. 29 shows similar results for the model without riser balcony. Forces are relatively small and there is a slight trend for the CFD to overestimate the maximum values despite of better agreement than the previous case. Repeatability does not seem largely influenced by the absence of the riser balcony when compared with the case previously shown, as the differences between these results for different water-shipping events and those with balcony are in the same order of magnitude.

Interestingly, as presented in Fig. 30(a), there may be a large variation of the elevation in the horizontal direction at the instant of peak force, such as in event 3, whereas the other events show smaller variation. In all cases, the station closest to the load cell, S1, shows the largest water elevation, which is expected due to the presence of the vertical wall. In a similar fashion, Fig. 30(b) shows the horizontal fluid velocity at each station at the instant of peak force from the CFD simulation. Event 3 differs substantially from the

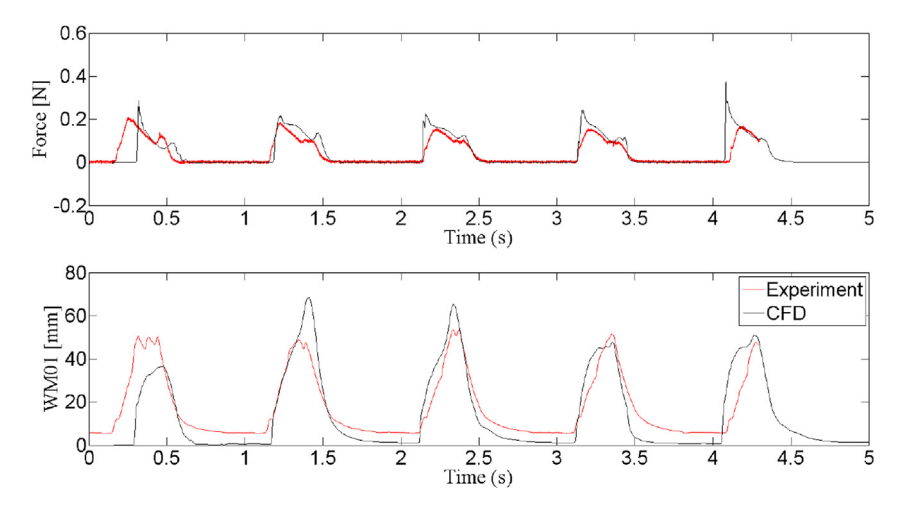


Fig. 36. Force time trace for the case with wave height 88 mm, period 0.97s. Set-up without riser balcony.

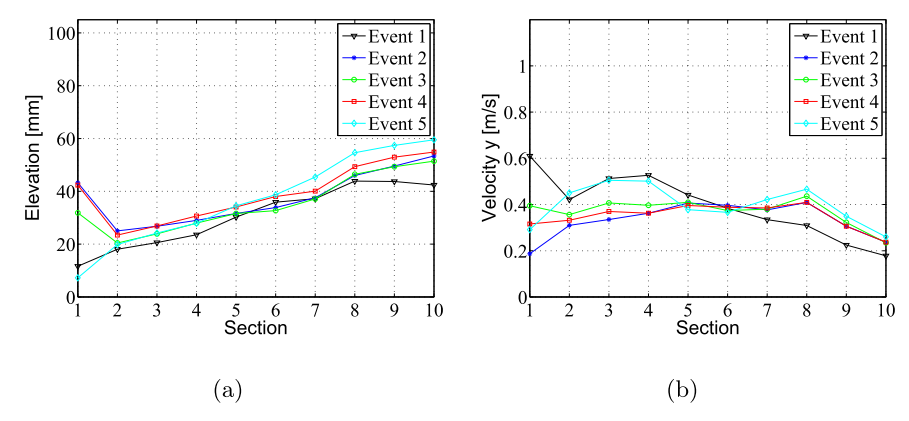


Fig. 37. Elevations (a) and Water horizontal mean velocity (b) at the moment of peak force for the case with wave height 88 mm, period 0.97 s at each of the ten stations. Setup without riser balcony.

others, but in all cases the velocity shows important variation over the horizontal coordinate.

Fig. 31 shows the evolution of the water over the deck until the moment of peak force in the last frame. A pattern similar to the dam-break type is once-again observed. Now, however, there is no evidence of significant air entrapment due to the absence of the riser-balcony. Fig. 32 shows a dam-break event type in the experiments.

# 5.2. Wave steepness 6%

#### 5.2.1. Case with riser balcony

Fig. 33 shows the force and water elevation time traces for the case with wave height 88 mm, wave period of 0.97s and with the riser balcony. These plots suggest weaker repeatability between cycles than the one seen for the cases with steepness 4%. The agreement in water elevation is now somewhat poorer and it is interesting to see that there is no clear correlation between the agreement of water level in each cycle and the one observed for the corresponding force measurements. Again, the force peaks obtained in the CFD simulations are generally more pronounced. Differently from the cases with 4% of steepness, the typical double-peak shape of the force trace is also observed in the experimental measurements. It is related to the fall of the water volume that previously ran upon the plate.

Fig. 34(a) shows the water elevations at the moment of peak force at the different stations on deck. Differently from the behavior observed for the 4% wave cases seen above, in this case, the maximum elevations occur at S10, decreasing to S4 and increasing again near the plate at S1. In Fig. 34(b), the horizontal velocity values are smaller near S10 and increase towards the plate.

In Fig. 35, the wave profile is presented for the fourth wave event by means of the volume fraction distribution. It is not clear whether the type of green water would be more similar to a dam break or a water-plunging type, called plunging wave + dam break by Ref. [10]. The water "folds" upon the balcony and a bubble is formed, after which the water column reaches the deck and then the load cell.

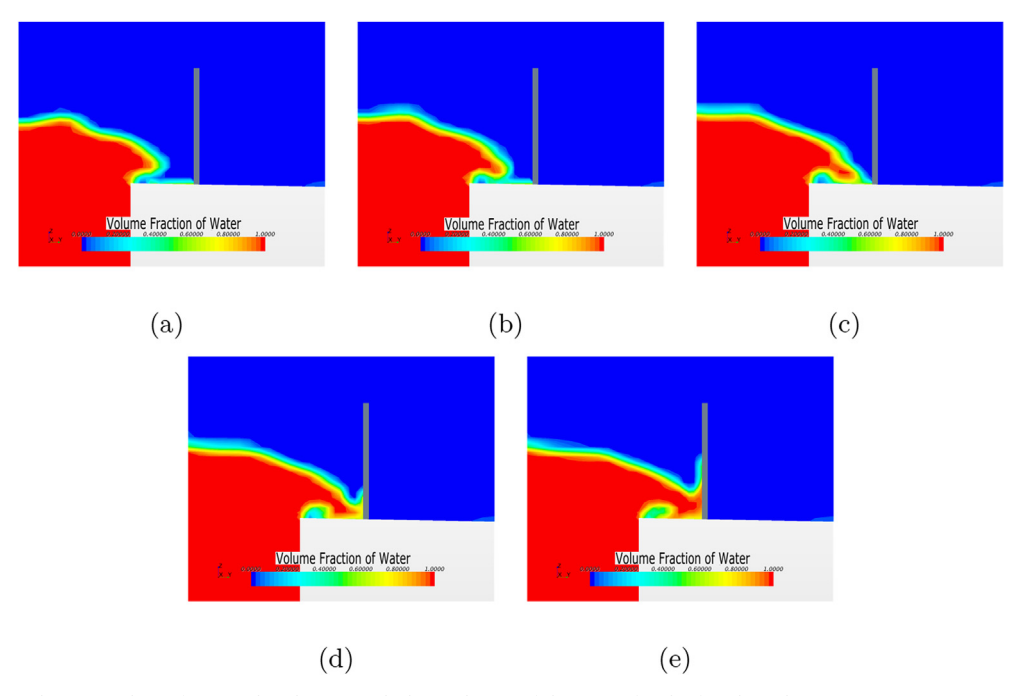


Fig. 38. Frames showing volume fraction distribution with the evolution of the water for the fourth peak. (a) $t_{peak} - t = 0.08s$ . (a) $t_{peak} - t = 0.08s$ . (b) $t_{peak} - t = 0.04s$ . (c) $t_{peak} - t = 0.02s$ . (e) $t_{peak} - t = 0.02s$ .

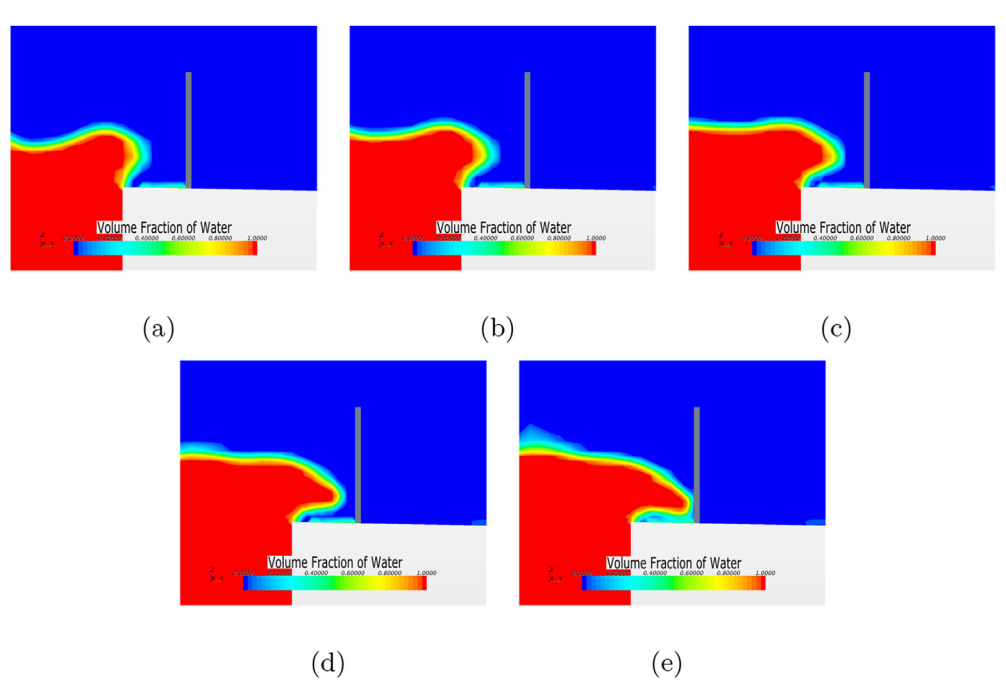


Fig. 39. Frames showing volume fraction distribution with the evolution of the water for the fifth peak. (a) $t_{peak} - t = 0.08s$ . (a) $t_{peak} - t = 0.06s$ . (b) $t_{peak} - t = 0.04s$ . (c) $t_{peak} - t = 0.02s$ . (e) $t_{peak}$ . Setup without riser balcony.

#### 5.2.2. Case without riser balcony

Fig. 36 shows similar results for the same wave and the model without riser balcony. The agreement obtained between CFD predictions and experimental measurements does not differs significantly from the one observed with the presence of the balcony. Actually, it could be anticipated that, as the wave amplitude increases, the influence of the balcony tends to become less pronounced. The water elevation distribution at the instant of the force peaks presented in Fig. 37(a) shows small differences among the different events. Fig. 37(b) shows the horizontal fluid velocity at each station and at the instant of peak force. Events 2, 3 and 4 show similar

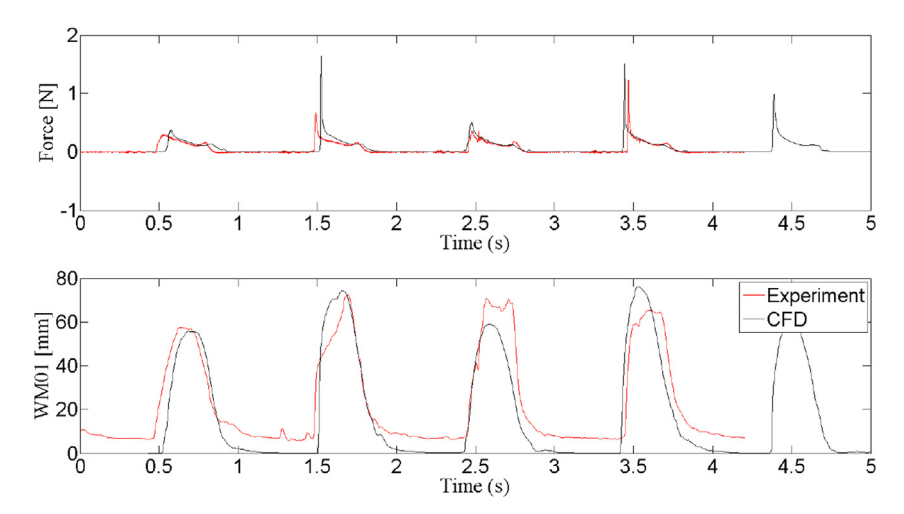


Fig. 40. Time traces of force (upper fig) and wave elevation (lower fig) for the case with wave height 117 mm, period 0.97s. Set-up with riser balcony.

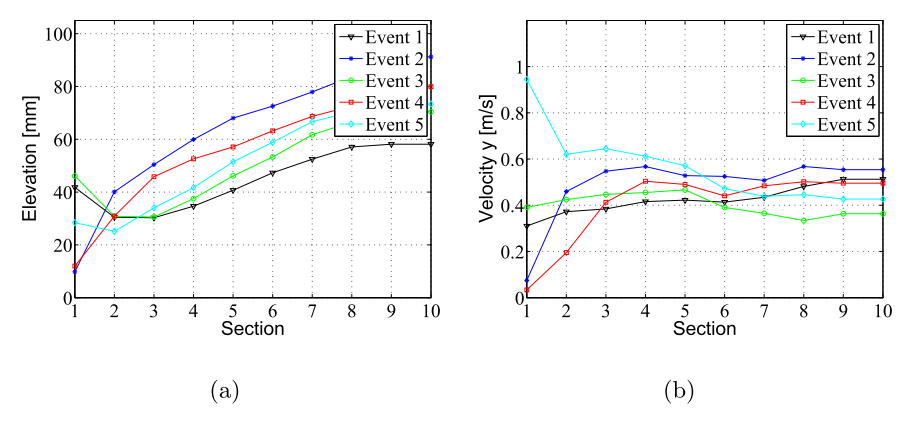


Fig. 41. Elevations (a) and Water horizontal mean velocity (b) at the moment of peak force for the case with wave height 117 mm, period 0.97 s at each of the ten stations. Set-up with riser balcony.

velocity distributions, which seem different from the distributions of events 1 and 5. Some further considerations on this point can be done based on the evolution of water profile.

In Figs. 38 and 39, the wave profile is presented respectively for the fourth and fifth wave events. In the first case, once again the water "folds" on the corner, after which the water column reaches the deck and then the load cell. In the other case, however, the water-plunging type is quite clear, with the water reaching the load cell directly, causing a larger impact force (as could be seen in the time-trace of Fig. 36). From these samples, it becomes quite clear that the slight variations in the water shipping from cycle to cycle lead to substantial differences in the impact forces.

#### 5.3. Wave steepness 8%

#### 5.3.1. Case with riser balcony

As it was observed in Fig. 18, the tests with the steepest waves (8%) where those that led to larger variability and also larger discrepancies between experimental and CFD results. It is, therefore, important to take a closer look in one sample case. Fig. 40 shows the force and elevation time trace for wave steepness 8% for the set-up with riser balcony. The comparison between experimental and numerical results is more difficult due to the strong non-linearity of the waves. There is large variability of the force peak amplitudes, highlighting the randomness of the phenomenon. Repeatability is quite weaker in this case, both for forces and wave heights.

Fig. 41(a) shows the elevation distribution at the moment of the force peaks, in which a large variation is observed among the different events with maximum elevations at the station S10 and a nearly monotonic decreasing behavior towards the plate. Fig. 41(b) shows that the horizontal fluid velocity distribution is also much less similar for the different events, especially when the water reaches the plate.

In Fig. 42, the progress of the water is presented for the second water shipping event. As observed with the 6% waves, in this case the event is of plunging-type with a large mass of water on deck reaching directly to the load cell, causing a more pronounced peak

G.F. Rosetti et al. Marine Structures 65 (2019) 154–180

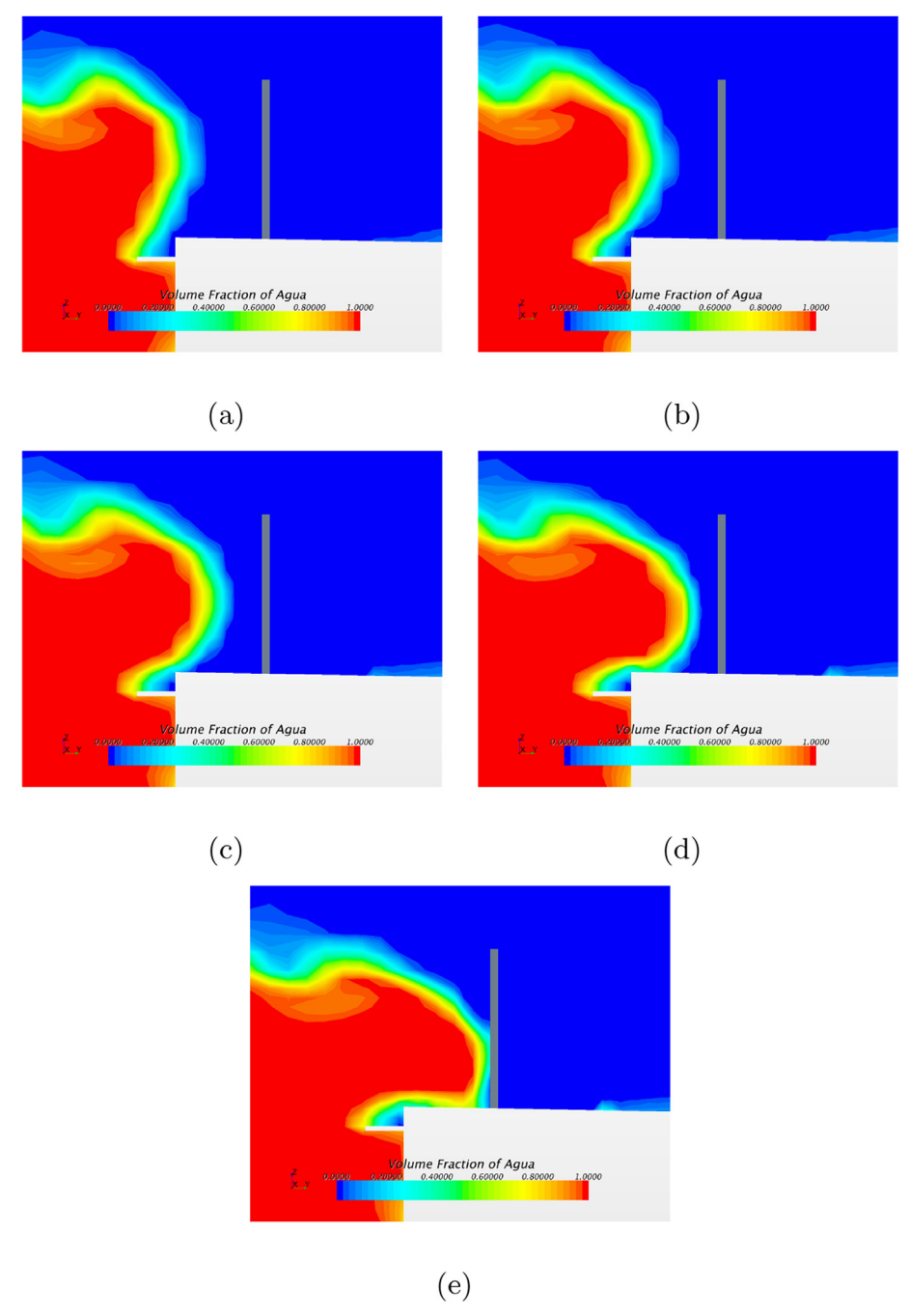


Fig. 42. Frames showing volume fraction distribution with the evolution of the water for the second peak. (a) $t_{peak} - t = 0.08s$ . (a) $t_{peak} - t = 0.08s$ . (b) $t_{peak} - t = 0.04s$ . (c) $t_{peak} - t = 0.02s$ . (e) $t_{peak}$ . Set-up with riser balcony.

for the impact force. Fig. 43 shows a plunging-type event in the experiments.

#### 5.3.2. Cases without riser balcony

Fig. 44 shows results for the same wave, now for the model without riser balcony. Interestingly, there is smaller variability of the force peak amplitudes and better comparison between experimental and numerical results. This, however, should not be generalized, even for other waves with the same steepness. Indeed, as previously shown in Fig. 18, waves with lower periods (and heights) again lead to larger variations and poorer agreement between CFD simulations and experiments.

Fig. 45(a) shows the elevation distribution at the moment of the force peaks, in which the second event shows different behavior when compared to the others. Consistently with this behavior, Fig. 45(b) shows that the horizontal fluid velocity distribution is most

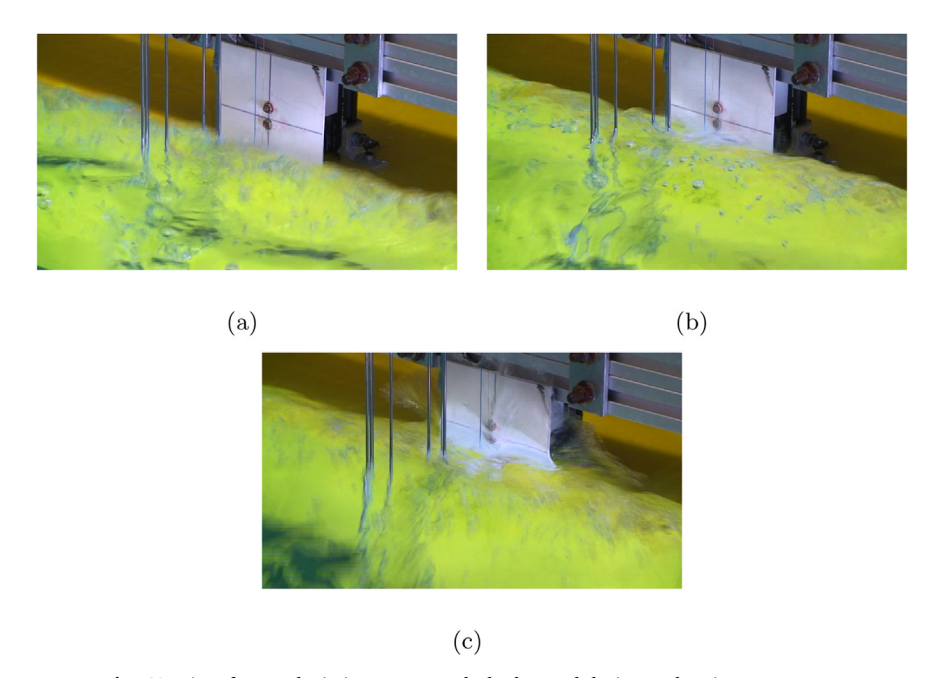


Fig. 43. Time frames depicting water on deck observed during a plunging-type event.

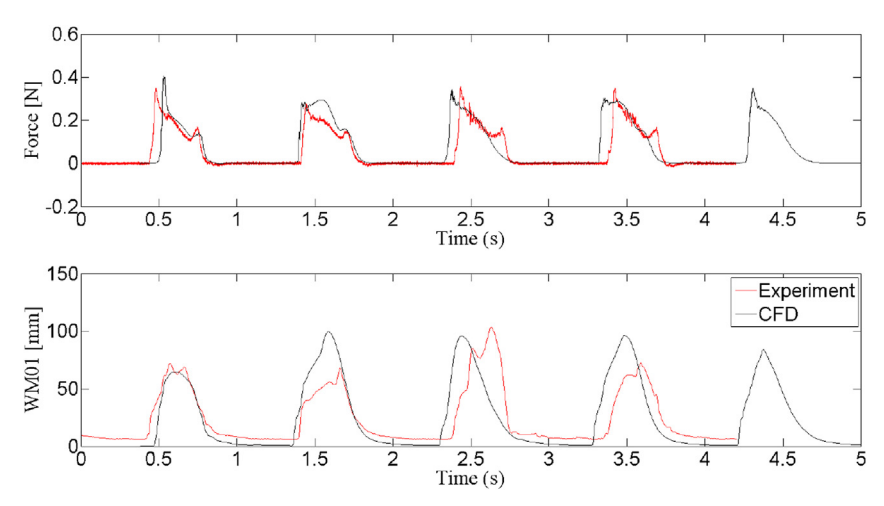


Fig. 44. Force time trace for the case with wave height 117 mm, period 0.969s. Setup without riser balcony.

different for the second event. This difference is consistently observed in the force time trace, when the peak force is less pronounced. In Fig. 46, the progress of the water is presented for the second water shipping event. In this case, it is a plunging-type event, because it hits the plate directly. Considering the severity of the impact event, the agreement between numerical and experimental results is actually remarkable.

# 6. Conclusions

An experimental analysis on green water events was executed in a wave flume with a fixed model representing the middle-body of an FPSO hull, emulating the incidence of beam waves on such structure. Water elevations and impact loads on a deck structure were measured and water velocities were calculated with the purpose of correlating this information. A range of regular waves was tested, with steepness 4%, 6% and 8%. The influence of a hull appendix emulating the upper part of a riser balcony was investigated both in the model tests and CFD simulations.

In general, a fair agreement was found between experiments and CFD calculations, both in terms of elevations and average of peak forces. In all cases, larger wave steepness was related to larger water loads and elevations; however, this was mostly associated with larger wave periods. The fixed model may explain these results, because in larger periods the model would follow the waves. The standard deviations of forces measured by the load cells showed weak correlation with wave steepness, wave heights or periods,

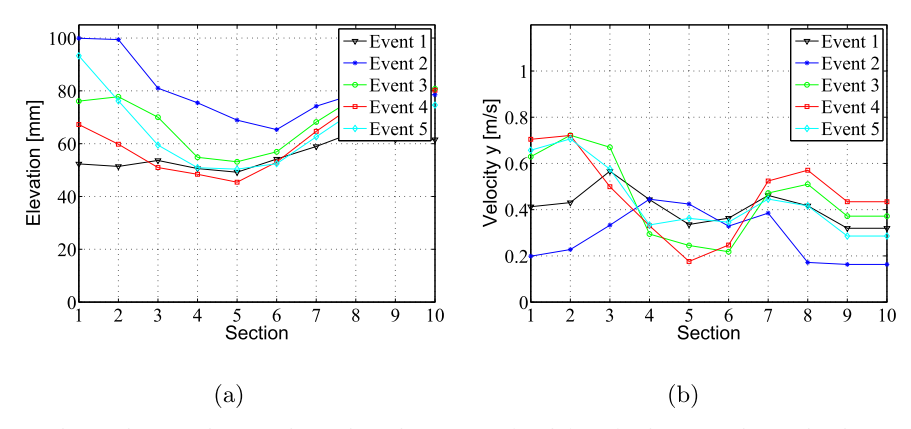


Fig. 45. Elevations (a) and Water horizontal mean velocity (b) at the moment of peak force for the case with wave height 117 mm, period 0.969 s at each of the ten stations. Setup without riser balcony.

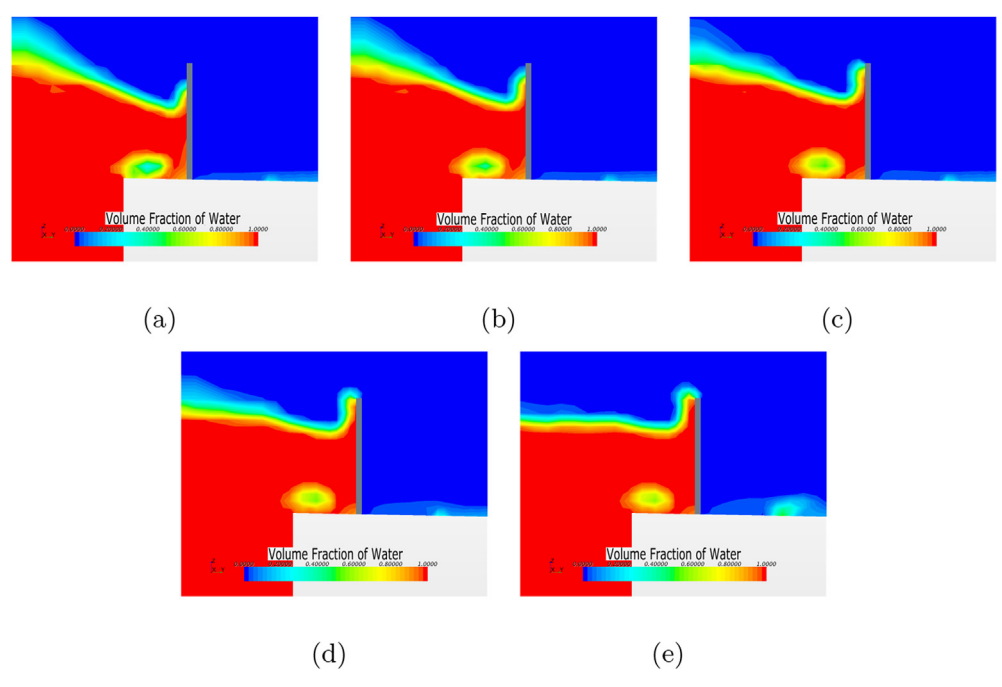


Fig. 46. Frames showing volume fraction distribution with the evolution of the water for the second peak. (a) $t_{peak} - t = 0.08s$ . (a) $t_{peak} - t = 0.08s$ . (b) $t_{peak} - t = 0.04s$ . (c) $t_{peak} - t = 0.02s$ . (e) $t_{peak}$ . Setup without riser balcony.

emphasizing the randomness of the water shipping events. In particular, the cases with wave steepness of 8% showed larger standard deviations than the other cases. As the water volume on deck is appreciable, somewhat larger spread of peak forces is observed.

There was not a clear relation between the presence of the riser balcony and the impact loads. In fact, in some cases the presence of the riser balcony even led to somewhat larger impact loads, which has to be seen taking into account that the riser balcony is placed near the free surface. Even though this is not the primary function of the riser balcony, changing its geometry and placing it at a larger height could be effective in attenuating the run-up.

In general, a weak correlation between velocities on deck and peak loads was found. This raises some questions regarding the validity of relating forces and water front velocities to determine empirical correlations that can be envisaged for water load predictions.

Closer observation of the flow for the different wave steepness led to the conclusion that little can be said regarding a consistent relation between elevations and velocities measured at a number of positions and the corresponding peak forces. Observation of the wave profiles showed that even waves with the same parameters (heights and periods) can display different behavior when subjected to minor changes of the local flow, thus resulting in different peak loads. This seems to be more relevant in steeper (and more nonlinear) waves.

In spite of the variability in the peak impact forces observed from cycle to cycle, the good agreement between mean values and deviation obtained in CFD and experiments attests that numerical model is able to capture the essence of the phenomena in a

G.F. Rosetti et al. Marine Structures 65 (2019) 154–180

statistical sense, thus being appropriate for an engineering analysis. In the same sense, it was shown that integral (force impulse) values obtained over a reasonable number of cycles and conditions could be predicted with very good agreement with respect to those obtained from the experimental measurements. In general, the CFD results observed in this study were conservative, which is meaningful considering the uncertainties that exist regarding the representativeness of the peak impact forces for subsequent structural analysis.

#### Acknowledgements

Authors gratefully acknowledge Petrobras for the financial support provided to this investigation under a broader R&D project on green water prediction on FPSOs. Alexandre Simos also acknowledges the Brazilian Research Council (CNPq) for his research grant.

#### References

- [1] Silva DFC. Avaliação Numérico-Experimental de Embarque de Água (Green Water) em FPSO Sujeito a Ondas Oblíquas e de Través PhD. thesis Universidade Federal do Rio de Janeiro; 2016. In Portuguese.
- [2] Silva DFC, Coutinho ALGA, Esperança PTT. Green water loads on FPSOs exposed to beam and quartering seas, Part I: experimental tests. Ocean Eng 2017;140:434–52.
- [3] Silva DFC, Esperança PTT, Coutinho ALGA. Green water loads on FPSOs exposed to beam and quartering seas, Part II: CFD simulations. Ocean Eng 2017:140:418-33.
- [4] Van't Veer R, Zuidscherwoude W. FPSO green water on deck assessment. International conference on violent flows, Nantes, France, September 25-27. 2012.
- [5] Xiao L, Yang J, Li X. An experimental investigation on wave runup along broadside of single point moored FPSO exposed to oblique waves. Ocean Eng 2014;88:81–90.
- [6] Ruggeri F, Watai RA, Mello PC, Sampaio CMP, Simos AN, Silva DFC. Fundamental green water study for head, beam and quartering seas for a simplified FPSO geometry using a mixed experimental and numerical approach. Mar Syst Ocean Technol 2015;10(2):71–90.
- [7] Östman A, Pakozdi C, Silva DFC. A fully non-linear RANS-VOF numerical wavetank applied in the analysis of green water on FPSO waves. Proceedings of the 2014 33rd international conference on ocean, offshore and artic engineering. 2014.
- [8] Lee HH, Lim HJ, Rhee SH. Experimental investigation of green water on deck for a CFD validation database. Ocean Eng 2012;42:47-60.
- [9] Buchner B. Green water on ship-type offshore structures PhD. thesis Technical University of Delft; 2002.
- [10] Greco M. A two-dimensional study of green-water loading PhD. thesis Norwegian University of Science and Technology; 2001.
- [11] Aureli F, Dazzi S, Maranzoni A, Mignosa P, Vacondio R. Experimental and numerical evaluation of the force due to the impact of a dam-break wave on a structure. Adv Water Resour 2015;76:29–42.
- [12] Pham XP, Varyani KS. Generic design of V-shape and vane type breakwaters to reduce green water load effects on deck structures and containers of ships: case study. J Waterway Port Coast Ocean Eng Jan/Feb 2006:57–65.
- [13] Silva DFC, Rossi RR. Green water loads determination for FPSO exposed to beam sea conditions. Proceedings of the 2014 33rd international conference on ocean, offshore and artic engineering, OMAE-24947, san Francisco, USA. 2014.
- [14] Loots E, Buchner B. Wave run up as important hydrodynamic issue for gravity based structures. Proceedings of the ASME 18th international conference on ocean, offshore and arctic engineering, OMAE2004-51084, vancouver, Canada. 2004.
- [15] Kleefsman KMT, Fekken G, Veldman AEP, Iwanowski B, Buchner B. A volume-of-fluid based simulation method for wave impact problems. J Comput Phys 2005;206:363–93.
- [16] Petrobras. Petrobras archives. 2014http://www.petrobras.com.br/fatos-e-dados/casco-da-plataforma-p-66-chega-a-angra-dos-reis.htm, Accessed date: 7 March 2017
- [17] ITTC. Experimentes on rarely occrring events recommended procedures and guidelines Technical Report 2011
- [18] Cd-Adapco. STAR-CCM + 9.06 documentation Technical Report 2016
- [19] Ferziger JH, Peric M. Computational methods for fluid dynamics, third ed. Springer Verlag; 2002.